Dissertation

submitted to the

Combined Faculty of Natural Sciences and Mathematics

of the Ruperto Carola University of Heidelberg, Germany

for the degree of

Doctor of Natural Sciences

Presented by

M.Sc. Diego Benusiglio

born in Turin, Italy

Oral examination: 10th September 2019

Somatosensory stimuli trigger coordinated oxytocin neurons activity during social interaction

Referees:

Prof. Dr. Valery Grinevich

Prof. Dr. Stephan Frings

Summary

The hypothalamic neuropeptide oxytocin (OT) promotes social communication via its central release in the mammalian brain. However, how social interaction affects electrical activity of OT neurons is still unclear. To address this question, I used cell-type specific viral vectors in combination with optoelectrode-based techniques. I performed the *in vivo* single-unit recording of optically identified OT neurons in the paraventricular nucleus (PVN) of hypothalamus in adult female rats during their social interactions with unfamiliar female conspecifics. Simultaneously, we monitored behavior and recorded ultrasonic vocalizations. The results showed that active social interactions events induce an increase of PVN OT neurons spiking activity as well as a re-organization of the firing pattern from regular to bursting. The action potentials of simultaneously recorded OT neurons were synchronized and phase-locked with the PVN theta oscillations precisely at the time of social interactions, but not during non-social exploratory behavior.

To decipher which sensory stimuli trigger OT neuron activity, I performed experiments with partial deprivation of specific sensory modalities. Direct physical contact between rats, or even gentle skin stimulation, led to a profound increase in OT firing rates. In contrast, presentation of visual, auditory and olfactory social-relevant stimuli alone did not significantly alter OT neuron activity. This led to the conclusion somatosensory component of social interaction drives OT neurons synchronous activity.

To further explore the effects of tactile stimuli on the OT system, I examined the expression of the marker of neuronal activity c-Fos after repetitive somatosensory stimulation; it appeared to be significantly increased in a particular subpopulation of OT neurons named parvocellular OT neurons. Employing *in-vivo* calcium recording via fiber photometry, I investigated the role of parvocellular OT neurons in regulating the activity of the general population of PVN OT neurons, finding that parvocellular OT neurons mediate the activation of the OT system in response to somatosensory stimuli. Next, I selectively modulated the activity of parvocellular OT neurons in awake freely moving rats via pharmacogenetics: activation of this population of neurons resulted in increased social interaction, while inhibition leaded to decrease of social interaction. Finally, I studied the effect of intracerebral infusion of an OT receptor antagonist which induced a substantial reduction of social interaction time, even when parvocellular OT neurons were activated.

Altogether, these results indicate that somatosensory stimulation is essential to activate OT neuron ensembles and, hence, can induce central neuropeptide release in socially interacting female rats. This opens perspectives for studying functional and anatomical

connectivity between the somatosensory and OT systems in normal and psychopathological conditions.

Zusammenfassung

Das hypothalamische Neuropeptid Oxytocin (OT) fördert soziale Kommunikation durch seine zentrale Ausschüttung im Gehirn von Säugetieren. Ungeklärt ist allerdings noch immer, wie soziale Interaktion sich auf die elektrische Aktivität von OT Neuronen auswirkt. Um diese Fragestellung zu untersuchen, verwendete ich Zelltyp-spezifische Virus Vektoren in Kombination mit Optoelektroden-basierten Techniken. Ich führte *in vivo* single-unit Aufnahmen von optisch identifizierten OT Neuronen im Paraventricular Nucleus (PVN) des Hypothalamus in adulten weiblichen Ratten während einer sozialen Interaktion mit einer unbekannten weiblichen Artgenossin durch. Gleichzeitig wurde das Verhalten überwacht und die Ultraschall Vokalisierung aufgezeichnet. Die Ergebnisse zeigten, dass aktive soziale Interaktion eine Erhöhung der Aktionspotential Frequenz der PVN OT Neurone sowie eine Reorganisation des Aktivitätsmusters von regulär zu gebündelt aktiv induziert. Genau zu den Zeiten, in denen soziale Interaktion stattfand, waren die Aktionspotentiale von gleichzeitig aufgenommenen OT Neuronen synchronisiert und Phasen-gekoppelt mit den PVN Theta Oszillationen, jedoch nicht während nicht-sozialem Erkundungsverhalten.

Um zu entschlüsseln, welche sensorischen Stimuli die Aktivität von OT Neuronen auslösen, führte ich Experimente durch, in denen eine partielle Deprivation von spezifischen sensorischen Modalitäten stattfand. Direkter körperlicher Kontakt zwischen Ratten oder sogar leichte Haut Stimulation führte zu einer hochgradigen Erhöhung der OT Neuron Aktionspotential Frequenz. Im Kontrast dazu änderten die Präsentation von visuellen, auditiven und olfaktorischen sozial relevanten Reizen alleine die Aktivität der OT Neurone nicht signifikant. Dies führte zu der Schlussfolgerung, dass die somatosensorische Komponente sozialer Interaktion die synchronisierte Aktivität der OT Neurone induziert.

Um die Effekte taktiler Stimulation des OT Systems noch weiter zu untersuchen, betrachtete ich die Expression des molekularen Markers für neuronale Aktivität c-Fos; sie schien in einer bestimmten Subpopulation von OT Neuronen, den parvozellulären OT Neuronen, signifikant erhöht zu sein. Unter Verwendung von Fiber Photometry für *in vivo* Calcium Messungen, erforschte ich die Rolle von parvozellulären OT Neuronen in der Regulation der Aktivität der generellen PVN OT Neuron Population und fand dabei heraus, dass parvozelluläre Neurone die Aktivierung des OT Systems als Reaktion auf somatosensorische Reize herbeiführen. Als Nächstes modulierte ich, pharmakogenetische Hilfsmittel nutzend, selektiv die Aktivität von parvozellulären OT Neuronen: Aktivierung dieser Population von Neuronen resultierte in einer erhöhten sozialen Interaktion, während Inhibition zu einer Verminderung der sozialen Interaktion führte. Schlussendlich untersuchte ich den Effekt intrazerebraler

Infusion eines OT Rezeptor Antagonisten, welcher eine substantielle Reduktion des sozialen Interaktionszeitraums herbeiführte, sogar wenn parvozelluläre OT Neurone aktiviert waren.

Zusammengefasst zeigen diese Ergebnisse, dass somatosensorische Stimulation essentiell ist um OT Neuron Ensembles zu aktivieren und somit die zentrale Ausschüttung von Neuropeptiden in sozial interagierenden weiblichen Ratten induzieren kann. Dies öffnet Perspektiven für die wissenschaftliche Untersuchung funktioneller und anatomischer Konnektivität zwischen den somatosensorischen und OT Systemen unter normalen und psychopathologischen Bedingungen.

List of abbreviations

AAV	Adeno-associated virus
AVP	Arginine-vasopressin
AN	Accessory nuclei of the hypothalamus
BBB	Blood brain barrier
BL	Blue-light
BNST	Bed nucleus of the stria terminalis
b.w.	body weight
Ca^{2+}	Calcium ion
CCK	Cholecystokinin
CeA	Central nucleus of the amygdala
ChR2	Channelrhodopsin 2
CNO	Clozapine-N-oxide
CNS	Central nervous system
CSI	Chambered social interaction
DIO	Double floxed inverted open reading frame
DREADD	Designer receptors exclusively activated by designer drugs
EYFP	Enhanced yellow fluorescent protein
FSI	Free social interaction
GABA	Gamma-aminobutyric acid
GECI	Genetically encoded calcium indicator
GFP	Green fluorescent protein
HEK cells	Human embryonic kidney cells
OT	Oxytocin
OTR	Oxytocin receptor
IGR	Intergenic region
ITR	Inverted terminal repeats
i.p.	Intraperitoneal
i.c.v.	Intracerebroventricular
LDCV	Large dense-core vesicles
PBS	Phosphate buffered saline
PCA	Principal component analysis

PFA	Paraformaldehyde
PSTH	Peri-stimulus time histogram
PVN	Paraventricular nucleus of the hypothalamus
rAAV	Recombinant adeno-associated virus
SI	Social interaction
SON	Supraoptic nucleus of the hypothalamus
SSV	Small synaptic vescicles
USV	Ultrasound vocalisation
VGluT2	Vesicular glutamate transporter 2
WPRE	Woodchuck hepatits virus posttranscriptional regulatory element

Table of Contents

Chapter 1: Introduction

1. Introduction

1.1. Oxytocin

The nine amino-acids cyclic neuropeptide oxytocin was first described in 1906 for its role in parturition and lactation (Lee *et al.*, 2010). The term oxytocin, derived from the Greek words (ωκνξ, τοκοκξ), means "quick birth" and was coined after the discovery of its uterine-contracting properties which facilitate parturition (Dale, 1906). For more than 50 years, oxytocin research focused on its peripheral roles in reproduction, delivery, and lactation. Only in the last decade researchers' attention have shifted on the possible roles that oxytocin has in the central nervous system. Oxytocin can be released peripherally into the blood stream via the posterior pituitary gland or centrally both from the dendrites and from the axons of OT neurons, which innervate numerous brain regions where oxytocin receptors are expressed. The functional role of oxytocin in the CNS has been involved in the regulation of a broad variety of social behaviors, such as social memory (Zhang *et al.*, 2016) and attachment, sexual and maternal behaviors (Neumann, 2008), and aggression (Veenema and Neumann, 2008), and non-social behaviors, including contextual learning (Hasan *et al.*, 2019), anxiety, feeding (Skinner *et al.*, 2019), and pain perception (Lee *et al.*, 2010).

The molecule oxytocin was the first neuropeptide to be synthesized in a laboratory thanks to the work of du Vigneaud and his team in the 50s (du Vigneaud *et al.*, 1954). It is composed of nine amino acids (Cys-Tyr-Ile-Gln-Asn-Cys-Pro-Leu-GlyNH_2) and its structure is very similar to another neuropeptide, arginine vasopressin (AVP), from which it differs by only two amino acids. Oxytocin, vasopressin and their homologues share common evolutionary history and their genomic sequences are well conserved across phyla (Caldwell and Young, 2006; Knobloch and Grinevich, 2014). The genes that encode for oxytocin and vasopressin are located closely in the same chromosome but are transcribed in opposite directions and are separated by an intergenic region (IGR) whose length varies across species (Caldwell *et al.*, 2008).

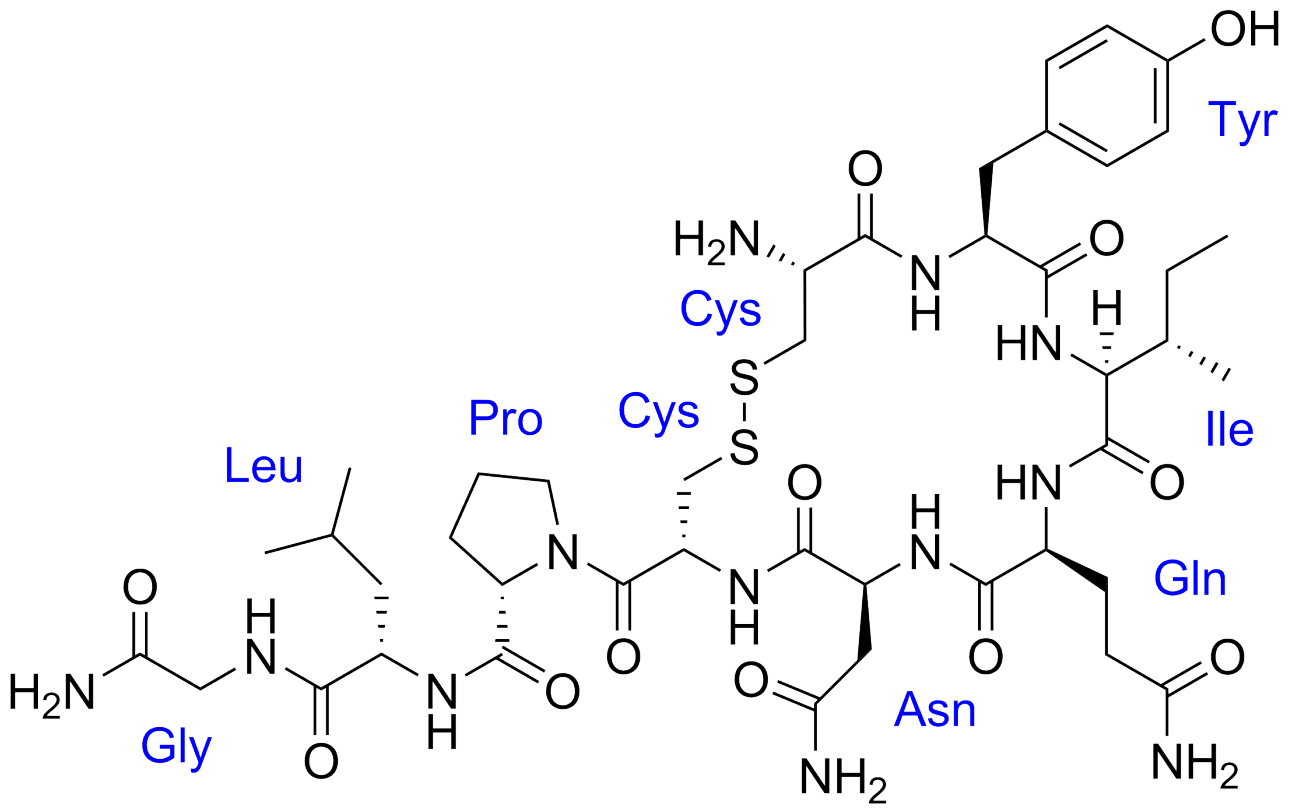

Figure 1.1 Chemical structure of oxytocin

Oxytocin is formed by nine amino acids in the sequence cysteine-tyrosine-isoleucine-glutamine-asparagine-cysteine-proline-leucine-glycine-amide (Cys-Tyr-Ile-Gln-Asn-Cys-Pro-Leu-GlyNH_2) with a sulfur bridge between the two cysteines that creates a cyclic six amino acid ring. Oxytocin is a large molecule with a molecular mass of 1007 Da and is not able to cross the blood-brain barrier; therefore, peripheral and central oxytocin concentrations can be independent. Oxytocin has only one receptor, the oxytocin receptor (OTR) which belongs to the rhodopsin-type (class I) G protein-coupled receptor (GPCR).

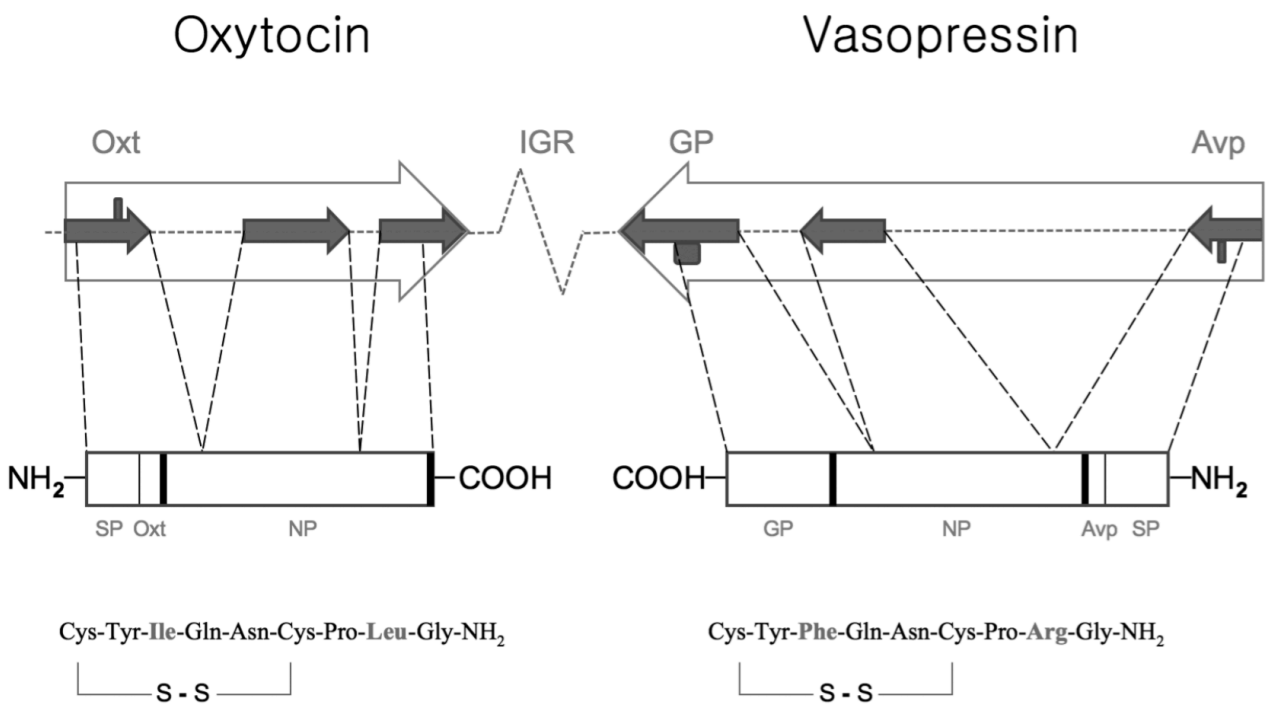

Figure 1.2 Diagram of the oxytocin and vasopressin genes.

Oxytocin and vasopressin genes (top, large arrows), preprohormones (middle, schematic boxes), and peptides (bottom). Both genes are formed by three exons (small black arrows) separated by two introns (dashed lines). The genes are located on the same chromosome but are transcribed in opposite directions and are separated by an intergenic region (IGR). The preprohormones are composed by a signal peptide (SP), a neuropeptide (OT or AVP), and a neurophysin (NP). In the case of AVP, it contains a glycopeptide (GP) as well. Adapted from (Caldwell et al., 2008).

1.2. Oxytocin neurons and the hypothalamus

In the mammalian brain oxytocin (OT) in synthetized, transported, and released by specialized endocrine neurons located in the paraventricular (PVN), supraoptic (SON), and accessory nuclei (AN) of the hypothalamus.

In the present work, we used female Wistar rats as a model for studying the action of oxytocin and the oxytocin neural system in a socially behaving animal. In the rat brain, the organization of oxytocin neurons in the hypothalamus looks as in the figure:

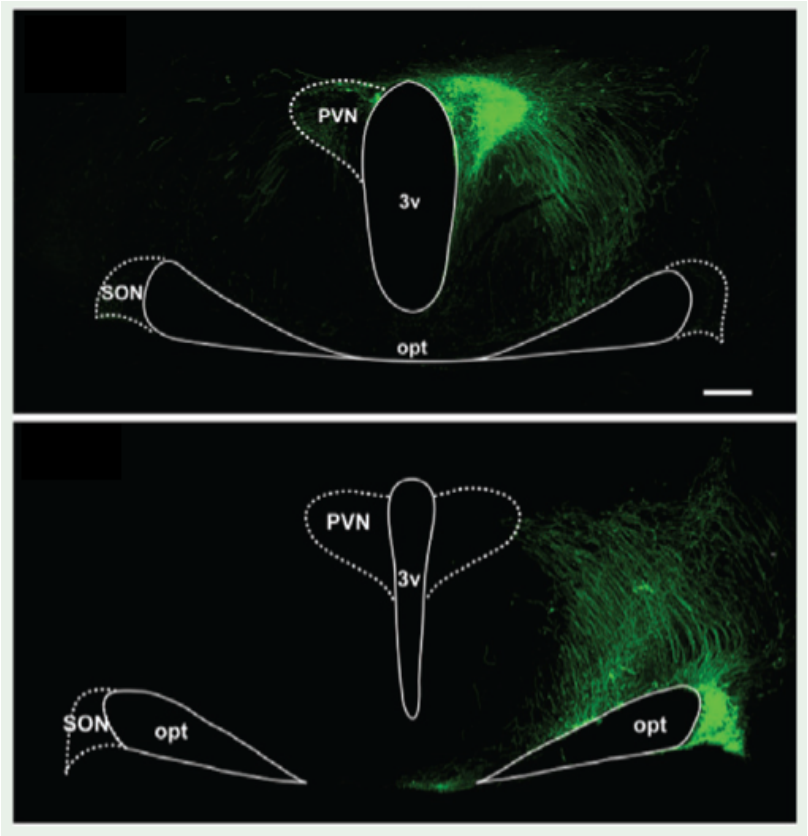

Figure 1.3 Oxytocin neurons location in the rat brain.
Coronal section of the rat hypothalamus. Oxytocin cells are infected with AAV OTp-Venus and appear in green color. On the top panel, the PVN is visible laterally to the third ventricle. On the bottom panel, the SON is located adjacently to the optic tract. A dense plexus of oxytocin-containing fibers connecting and arising from the two nuclei are clearly visible. Scale bar 200 μm. Adapted from (Eliava et al., 2016).

The total number of oxytocin-positive cells in the rat brain has been estimated to be around 8000. About 2400 oxytocin cells reside in the PVN of hypothalamus, approximately 4000 in the SON, 1000-1200 in the AN, and 700 in the anterior commissural nucleus (Rhodes, Morriell and Pfaff, 1981; Althammer and Grinevich, 2018). Those cells can be divided in two anatomically and functionally distinct cell types: the magnocellular and parvocellular oxytocin neurons (Swanson and Kuypers, 1980; Swanson and Sawchenko, 1980; Althammer and Grinevich, 2018).

1.2.1. Magnocellular neurons

Magnocellular oxytocin neurons are large endocrine cells (diameter of somas 20-30 μm), which can be found in all three hypothalamic nuclei PVN, SON, and AN. Each magnocellular neuron sends one axon/varicosity to the posterior pituitary gland, where oxytocin is released into the blood stream. Axon collaterals of magnocellular OT neurons also project to various forebrain regions, including the central nucleus of the amygdala (Knobloch *et al.*, 2012), lateral septum (Menon *et al.*, 2018), nucleus accumbens (Amadei *et al.*, 2017), hippocampus (Smith *et al.*, 2016), and medial prefrontal cortex (Sabihi *et al.*, 2014), where OT receptors have been found. Stimulation of endogenous OT axonal release in these regions, e.g. by

optogenetics, modulates contextual fear (Knobloch *et al.*, 2012), anxiety-related behavior (Jurek and Neumann, 2018) as well as olfactory-dependent social recognition (Oettl *et al.*, 2016). Projections of magnocellular oxytocin neurons have also been in found in some hindbrain region such as the ventral tegmental area, a key node in the reward circuitry, where oxytocin release is necessary to elicit social reward (Hung *et al.*, 2017).

In addition to axonal peptide release, magnocellular oxytocin neurons also display somato-dendritic release, a mechanism that provides local feedback signal that allows oxytocin neurons, which also express OT receptors, to synchronize their firing activity leading to pulsatile OT secretion during lactation (Ludwig and Leng, 2006; Tobin, Leng and Ludwig, 2012).

Finally, some magnocellular oxytocin neurons can also be found in close proximity to the third ventricle where they release oxytocin into the cerebrospinal fluid for intra-brain circulation (Engelmann *et al.*, 1999).

1.2.2. Parvocellular neurons

Parvocellular oxytocin neurons are smaller than magnocellular neurons (diameter of somas is ~ 10-20 μm) and are mainly located in the caudal portion of the PVN (Swanson and Kuypers, 1980). In contrast to magnocellular neurons, parvocellular neurons do not send axons to the posterior pituitary; however, they send axons to the brainstem and the spinal cord (Swanson and Sawchenko, 1980), where they modulate a variety of physiological functions, such as breathing (Mack *et al.*, 2002), erection and copulation (Melis, Argiolas and Gessa, 1986), cardiovascular reactions such as blood pressure and heart rate (Petersson, 2002), gastric reflexes and food intake regulation (Sabatier, Leng and Menzies, 2013), and pain perception (Rash, Aguirre-Camacho and Campbell, 2014).

OT-ergic projections arising from parvocellular neurons have been found in several hindbrain regions such as the periaqueductal grey (PAG) (Juif and Poisbeau, 2013), hypoglossal nucleus of the medulla (Wrobel *et al.*, 2010), brainstem (Blevins, 2004), nucleus tractus solitarii (NTS) (Ho *et al.*, 2014), and in the spinal cord (Tribollet, Barberis and Arsenijevic, 1997).

Parvocellular neurons have been proven to regulate the activity of magnocellular neurons via PVN-SON connections (Eliava *et al.*, 2016) and their total number in the rat brain has been estimated to be between 70 and 200 cells, accounting approximately for 1 % of the total population of oxytocin neurons (Althammer and Grinevich, 2018).

Several tools are available to discriminate between magnocellular and parvocellular neurons; the most widely used is via i.p. application of hydroxystilbamidine (known as “Fluorogold”). After systemic injection, Fluorogold is uptaken by terminals of magnocellular neurons in the pituitary, from where it is retrogradely transported to the cell bodies. By contrast, parvocellular neurons do not have any projection outside of the BBB, and therefore will not contain any Fluorogold. Immunostaining with fluorescent antibodies against Fluorogold and against oxytocin eventually allows to distinguish the two cell types.

1.3. Electrical properties of oxytocin neurons and peptide release

Oxytocin neurons are electrically excitable and they generate action potentials in response to afferent inputs and thereby triggering neuropeptide release. Oxytocin can be released systemically through the posterior pituitary gland, or centrally through distinct mechanisms. The large precursor molecules of oxytocin are stored in large dense core vesicles (LDCVs) which are produced exclusively in the cell body of oxytocin neurons and subsequently distributed throughout the soma, dendrites, and axons of oxytocin neurons. In response to increased intracellular Ca^{2+} concentrations the LDCVs fuse to the cellular membrane and are exocytosed in order to release the peptide molecules outside of the cell (Stoop, 2012). LDCVs are different from other classes of neurotransmitter vesicles, like the small synaptic vesicles (SSVs), which are the primary vehicles for classical neurotransmitters such as glutamate or GABA. The release of SSVs is generally restricted to the synaptic cleft or to highly specialized membrane structures; conversely, LDCVs are broadly distributed and they can be release from any part of the neuron, including the cell body, dendrites, and axon (Ludwig *et al.*, 2002). In contrast to classical neurotransmitters contained in SSVs, whose action is limited to a small area in the proximity of the release site, large neuropeptides such as oxytocin can diffuse in a much larger volume. Considering that a single LDCV contains up to 85.000 molecules of oxytocin (Nordmann and Morris, 1984), it has been estimated that the release of one vesicle from an axon produces a concentration of oxytocin sufficient to activate oxytocin receptors (1nM, 50% effective OTR occupancy) in a spherical volume of 55 μm radius; the release of 10 vesicles is expected to result in an effective volume of 120 μm radius (Chini, Verhage and Grinevich, 2017).

The largest amount of oxytocin is transported by axons of magnocellular oxytocin neurons and released into the blood circulation via the posterior pituitary gland. Collateral innervations of these same axons reach various forebrain regions, where oxytocin is released *en passant* to modulate and facilitate a plethora of different behaviors (Knobloch

et al., 2012). The very same axon collaterals may also release glutamate from synaptic terminals since VGluT2 is co-expressed with oxytocin. In contrast to magnocellular neurons, parvocellular oxytocin neurons, that do not project to the posterior pituitary gland, directly innervate various midbrain and hindbrain regions as well as some portion of the spinal cord. In addition to axonal release, somato-dendritic exocytocis of oxytocin into the extracellular space allows peptide diffusion to hypothalamic sites (Ludwig *et al.*, 2002) and can contribute to the synchronization of neuronal activity: oxytocin neurons express oxytocin receptors allowing for an auto-excitatory positive feedback loop (Johnson and Young, 2017). This synchronization is required for pulsatile peptide release into the periphery in response to robust osmotic or reproductive stimuli, such as parturition and milk ejection. Finally, dendritic innervation of the third ventricle may allow oxytocin release into the ventricular circulation (Knobloch and Grinevich, 2014).

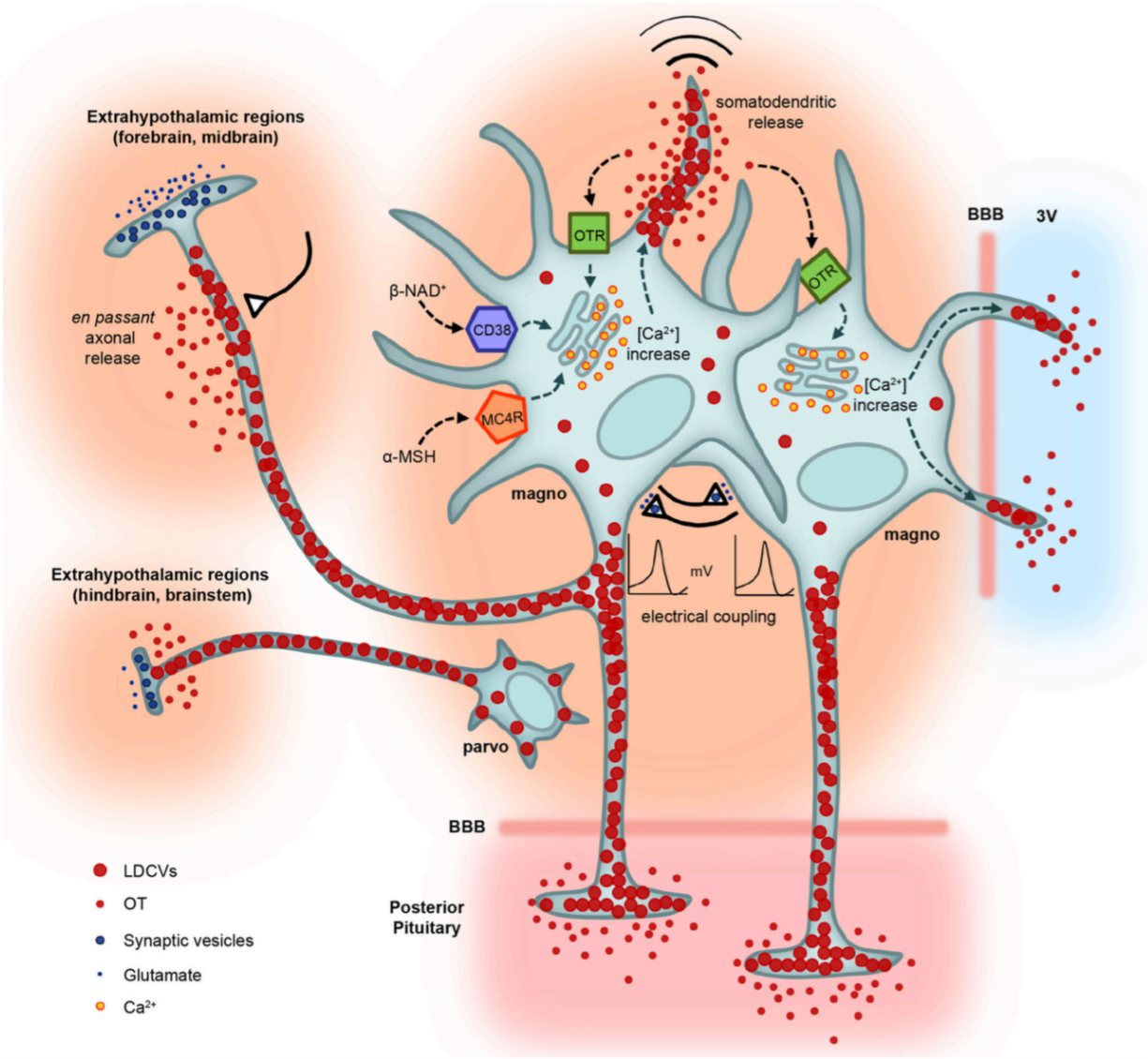

Figure 1.4 Oxytocin neurons morphology, projections, and peptide release mechanisms.

Schematic representation of oxytocin neurons structure and function. Magnocellular and parvocellular oxytocin neurons project to different targets. Magnocellular oxytocin neurons project to posterior pituitary and, via collaterals, to extrahypothalamic forebrain and midbrain regions, where oxytocin is released en passant. Dendrites of magnocellular neurons can also contact the third ventricle and release oxytocin into the cerebrospinal fluid. By contrast, parvocellular oxytocin neurons project predominantly to the hindbrain, to the brainstem, and to the spinal cord. Axons collaterals from some parvocellular oxytocin neurons can synapse onto and excite magnocellular oxytocin neurons in the SON. Somato-dendritic exocytosis of LDCVs allows oxytocin to diffuse locally where it can bind to auto-receptors and prime oxytocin neurons for firing. Glutamatergic connections between magnocellular oxytocin neurons generate an auto-excitatory network that synchronizes oxytocin neurons firing and leads to pulsatile oxytocin release into the periphery. Adapted from (Johnson and Young, 2017).

1.4. Effects of central oxytocin release

Oxytocin is involved in the modulation of a large spectrum of behaviors, which are often interlaced. Studies that monitored local extracellular concentrations of oxytocin by intracerebral microdialysis reported increased oxytocin release during social behaviors in rodents (Veenema and Neumann, 2008). In consistence with that, intracerebral administration of oxytocin or oxytocin agonists has been linked to increase of pro-social and affiliative behavior (Lee *et al.*, 2010); by contrast, infusion of oxytocin receptor antagonist into the brain is associated with decreased social behavior (Dumais *et al.*, 2013; Dumais, Alonso, Immormino, *et al.*, 2016); however, these effects are often region-, sex-, and dose-specific.

Oxytocin action in the brain is involved in many aspects of social behaviors, such as social recognition and discrimination, social memory, parenting, aggression across different species (Lee *et al.*, 2010). For example, in male rats infusion of oxytocin in the lateral ventricles enhances social recognition 2 hours after the first encounter with a novel conspecific (Benelli *et al.*, 1995), suggesting a role for oxytocin in the acquisition phase. I.c.v. (intracerebroventricular) administration of an oxytocin antagonist (AOVT) impairs social recognition in females rats (Engelmann *et al.*, 1998). Effects of oxytocin administration are usually brain region specific: e.g. OT injection into the medial preoptic area of the

hypothalamus (mPOA) facilitates social recognition, but it does not when injected in the septum (Popik and van Ree, 1991). Affiliative behaviors, such as formation of social bonds and pair bonding, and sexual behaviors are species-specific (Carter 1998) and are facilitated by oxytocin administration.

In the recent years, oxytocin has reported a growing interest also outside of the scientific community for the potential effect of oxytocin in increasing social trust in humans (Kosfeld *et al.*, 2005).

In conjunction to its effects on social behaviors, oxytocin is also involved in the regulation of non-social behaviors such as non-social memory (Lee *et al.*, 2010), stress and anxiety (Neumann *et al.*, 2000; Neumann, 2002; Neumann and Landgraf, 2012), fear expression and fear extinction (Hasan *et al.*, 2019).

1.5. Oxytocin and sensory systems

The effects of the neuropeptide oxytocin on the brain are often associated with social behaviors. At the same time, the ability to interact with conspecifics through complex social behaviors require detection and response to cues coming from multiple sensory modalities (Chen and Hong, 2018). In the mammalian brain, oxytocin receptors have been found in several forebrain regions involved in perception and sensory processing, therefore numerous studies (for a review see (Grinevich and Stoop, 2018)) have been focusing on the relationship between oxytocin and the sensory systems.

Already very shortly after birth, during early development, oxytocin plays an important role in the formation of infant-parent bonding, and this is may also suggest that oxytocin can affect the development of sensory systems. Throughout development, various regions of the brain undergo critical periods of plasticity that can be opened and closed by changes in the Excitation/Inhibition (E/I) balance of a particular neural circuit. Intriguing, oxytocin is known to affect the E/I balance in the hippocampus, where it increases the local network signal-to-noise ratio and enhances sensitivity to external stimuli (Owen *et al.*, 2013); oxytocin also affects the E/I balance in the central nucleus of the amygdala (Huber, Veinante and Stoop, 2005; Stoop, Hegoburu and van den Burg, 2015), where it modulates autonomic fear response. Finally, has been shown that oxytocin release is necessary for processing of social relevant stimuli in the auditory cortex (Marlin *et al.*, 2015) and in the olfactory system (Wacker and Ludwig, 2012).

It is clear that oxytocin plays an important role on neurotransmission and development in various brain regions involved in sensory processing; by contrast, there is only limited

knowledge on whether and how oxytocin neurons activity and oxytocin signaling is affected and modulated by sensory inputs.

1.5.1. Oxytocin and the somatosensory system

Oxytocin can be released in response to both noxious (painful) and non-noxious (pleasant) somatosensory stimulation. Central oxytocin release in response to painful and stressful stimuli can contribute to mitigate the stress reactions and alleviate the pain: a particular attention in this research field is dedicated to the effects of oxytocin on somatosensory signaling due to the strong analgesic action of the neuropeptide (Eliava *et al.*, 2016; Boll *et al.*, 2017).

During labor and breastfeeding oxytocin is released into the blood stream in response to sensory stimulation coming from peripheral nerves: the release is triggered by the activation of sensory nerves coming from the urogenital tract (pelvic/hypogastric nerves) and from the nipples (mammary nerves), and it induces uterine contraction and milk ejection respectively. Oxytocin can be released also following low intensity non-noxious stimulation of the skin or the hair through “activation of cutaneous sensory nerves in response to touch, light pressure, massage-like stroking, warm temperature and by low intensity electrical stimulation of sensory nerves in rats” (Uvnäs-Moberg, Handlin and Petersson, 2015). For example, oxytocin plasma levels are increased after 10 minutes of gentle stroking in male rats (Stock and Uvnäs-Morbeg, 1988).

A recent study by (Walker *et al.*, 2017) suggests that a particular class of touch sensitive nerve C fibers, named C-tactile afferents, may be responsible to mediate oxytocin release during affiliative tactile interactions. In fact, C-tactile afferents are unmyelinated, low threshold, pain unsensitive mechanoreceptors that respond optimally to low intensity and low speed stroking or gentle touching and are thought to be evolved in mammals to signal the rewarding value of physical contacts during social interactions.

1.6. Optogenetics

Optogenetics is the use of light-activated ion channel proteins to control neuronal function of a genetically restricted cell population. The main advantage of optogenetics is the ability to activate specific neurons that are embedded in a heterogeneous cell environment (Britt, McDevitt and Bonci, 2012). To achieve this specificity, optical actuators such as Channelrhodopis (ChR), Halorhodopsin (HR) or Achaerhodopsin (BR/PR) are expressed in the cell population of interest through viral vectors.

The most common excitatory light-sensitive protein used nowadays is channelrhodopsin-2 (ChR2), a cation channel which has been extracted from an algal protein from the specie *Chlamydomonas reinhardtii*. ChR2 is cable of transducing short flashes of blue light into spiking activity with high temporal (millisecond) resolution. Stimulation with light of defined wavelength (~470 nm for ChR2) triggers the cation channel to undergo a conformational change that lead to influx of cations (Ca^{2+}, Na^{2+}, H^{+}) inside the cell cytoplasm. This results in a depolarization of the cells that triggers the initiation of one or more action potentials (Yizhar *et al.*, 2011).

In the present study, I employed the optogenetic technique to identify and sort oxytocinergic cells among the population of extracellularly recorded PVN neurons.

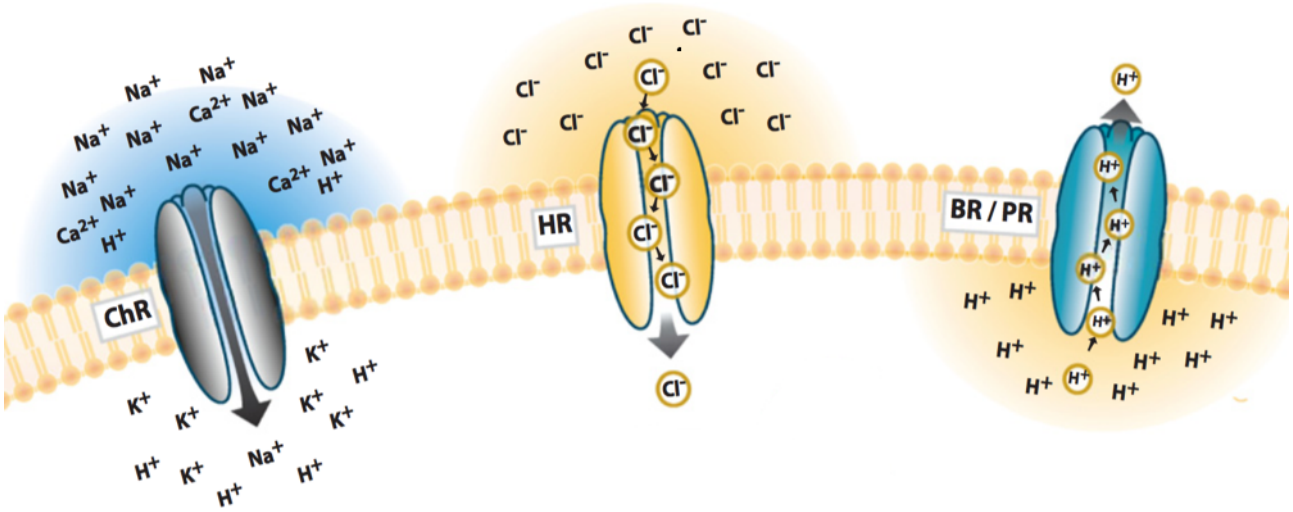

Figure 1.5 Light activated ion-channels.

Illustration of single-component optogenetic tools: plasma membrane-bound ion pumps and ion channels and transported ions.

***Left**: activation of the cation channel channelrhodopsin (ChR) by blue light (maximal absorption wavelength ~ 480 nm) generates a flux of positive ions inside the cytoplasm resulting in depolarization of the cell. **Center**: light-activated (maximal absorption wavelength ~ 570 nm) chloride pump halorhodopsin (HR) actively transports Cl^- inside the plasma membrane causing a hyperpolarization of the cell. **Right**: the proton pump bacteriorhodopsin (BR/PR) forces protons from the cytoplasm to the extracellular space resulting in hyperpolarization of the cell. Adapted from (Yizhar et al., 2011).*

1.7. Pharmacogenetics (DREADD) modulation of oxytocin neurons

The pharmacogenetic technology DREADD (Designer Receptors Exclusively Activated by Designer Drugs) is a well-established tool to manipulate neuronal and non-neuronal cell activity in freely moving animals (Roth, 2016). The DREADD systems are based on “Designer Receptors”, the mutated human muscarinic receptors hM3Dq and hM4Di which are uniquely activated by the “Designer Drug” clozapine-N-oxide (CNO), but are not activated by any endogenous neurotransmitter. At the same time, CNO is a pharmacologically and behaviorally inert molecule in absence of the designer receptors (when administered at the recommend dose, generally from 0.1 to 3 mg/kg). Moreover, CNO can be easily injected systemically or intraperitoneally, it has good drug-like properties such as rapid CNS penetration and distribution and it has a half-life time in the organism of roughly 2 hours (110±8 min, according to (Aitchison *et al.*, 2000)) that is suitable for many behavioral experiments.

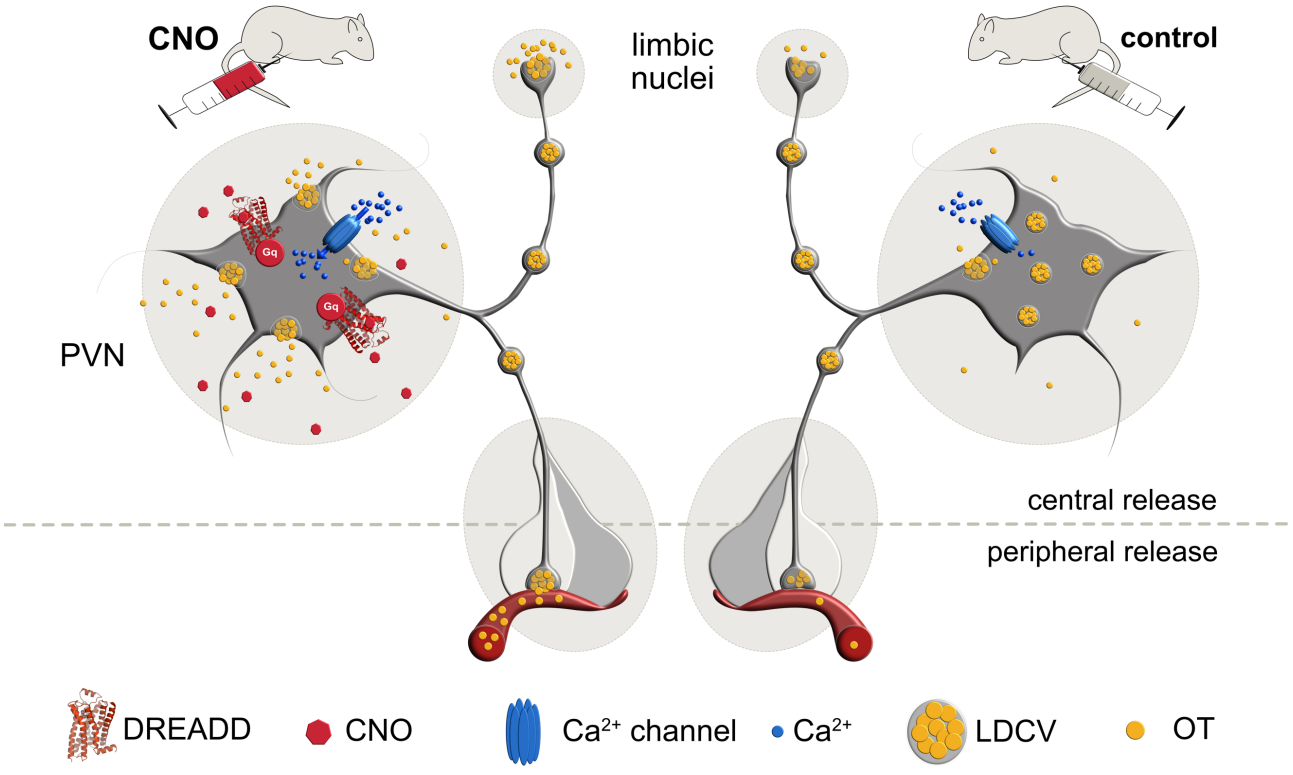

Figure 1.6 Cell type-specific activation of oxytocin neurons by chemogenetics.
Oxytocin neurons transfected with adeno-associated viruses (left panel) that induce the expression of designer receptors (DREADD) on the plasma membrane compared to control non-transfected oxytocin neurons (right panel). Specific activation of oxytocin neurons is mediated by i.p. injection of the DREADD agonist clozapine-N-oxide (CNO). Binding of

clozapine to the receptors cause a Gq-mediated Ca^{2+} influx into the cell. The increase of intracellular Ca2+ concentration inside the cell evokes the fusion of oxytocin containing large dense-core vesicles (LDCVs) to the plasma membrane and release of their content into the extracellular space. The release of oxytocin occurs from the somato-dendritic compartment, as well from the axons in distant forebrain regions and from the terminals in the neurohypophysis. Adapted from (Grund et al., 2019).

1.7.1. Gq-DREADD and Gi-DREADD

The mutated human muscarinic receptors hM3Dq and hM4Di belong to the family of GPCR (G-protein coupled receptors). When activated by the presence of CNO, hM3Dq increases the neuronal firing by activating the Gq signaling in the cell and is therefore named as a Gq-coupled DREADD. By contrast, CNO-mediated activation of hM4Di decreases the neuronal firing and inhibit presynaptic activity by acting of the Gi signaling and is named as Gi-coupled DREADD.

1.7.2. Oxytocin neurons modulation by DREADD system

Oxytocin neuron specific expression of hM3Dq or hM4Di is achieved by injection of rAAV carrying the sequence to express the DREADD proteins under the control of the oxytocin promoter. After viral injection, and after three weeks of viral expression, the protein of interest is expressed exclusively in oxytocin neurons and CNO administration will specifically increase (hM3Dq) or suppress (hM4Di) neuronal firing in this type of cells. Timing and dosage for optimal CNO administration in rats for behavioral testing are described in (Grund *et al.*, 2019).

1.8. Genetic markers of neuronal activity c-*fos*

The immediate early gene, c-*fos*, and its protein product, Fos, have been used as a tool for determining changes in neuronal activity for more than 30 years (Sagar, Sharp and Curran, 1988). In this early work from Sagar *et al*., authors show a significant increase in Fos immunostaining in the rat motor and sensory cortex of rats whose hindlimbs were electrically stimulated; secondly, they show a very pronounced increase in Fos expression in the PVN and SON of rats that were deprived of water for 24 hours. The gene c-*fos* is rapidly and transiently expressed in neurons after synaptic stimulation, i.e. when the electrical activity of the neuron changes from its resting state. Since the expression of Fos in basal conditions is relatively low in most of the CNS, immunostaining of Fos provides a useful technique to

map functional activity of neurons in a brain-wide manner. Moreover, the fact that c-Fos immunoreactivity is exclusively nuclear further allows double-labelling with other neurotransmitters localized in the cytoplasm. This feature is essential for studying the activity of neuroendocrine neurons which are diffusely distributed in regions containing multiple neuronal types (Ceccatelli *et al.*, 1989).

Even though Fos immunostaining is widely used and reliable technique to identify neuronal activity, increased neuronal firing does not always equals increased Fos expression; is the changes in signal transduction pathways that induce c-*fos* expression, not cell depolarization itself, therefore some precautions need to be taken when drawing conclusions based on this method (Hoffman and Lyo, 2002).

1.8.1. c-Fos expression in oxytocin neurons

Expression of c-*fos* of oxytocin neurons in basal condition is very low, such that no immunoreactivity is usually detectable in any oxytocin cells, unless its expression is increased by some physiological challenges such as water deprivation (citation here), salt loading, or exposure to fearful or stressful stimuli (e.g. foot shocks) (Hasan *et al.*, 2019).

An interesting property of the oxytocin neural system is that, in certain condition such as lactation or parturition, peptide release can be drastically enhanced by changing the neuronal firing pattern from regular to bursting, leading to pulsatile release of oxytocin into the pituitary (Rossoni *et al.*, 2008). This firing pattern reorganization however does not increase significantly the average number of action potentials discharged over time and therefore does not induce a robust increase of Fos expression in oxytocin cells. Interestingly, in lactating rats, oxytocin neurons do not display Fos immunoreactivity as in basal condition, even though large amounts of oxytocin are released following neuronal bursting to induce the milk ejection reflex. In conclusion, it seems that, in oxytocin neurons, c-*fos* expression is linked to steady increase of firing activity, but it is unsensible to changing in firing patterns that do not affect the average number of action potentials discharged over time.

Chapter 2: Methods

2. Methods

2.1. Animals

Experiments were performed with 4 to 8-week old virgin female Wistar rats, which were purchased from Janvier Labs (France). In total, 109 rats were used, of which 13 were excluded from analysis due to mistargeting or insufficient expression of viral vectors. The animal experiments were approved by the Committee on Animal Health and Care of the Government of Baden-Württemberg. All animals had *ad libitum* access to both water and food during the time in their home cages.

2.2. Viruses (rAAVs)

Several recombinant adeno-associated viruses (rAAVs) have been used in the experiments described in this thesis: six different rAAV vectors had been used, as summarized in Table 2.1. All genes of interest were cloned into a rAAV serotype 1/2 viral backbone.

Table 2.1 rAAV vectors

# Number	rAAV contruct name
1	OTp - ChR2 - mCherry
2	OTp - GCaMP6s
3	OTp-mCherry
4	OTp - DIO - GFP
5	OTp - DIO - hM4D(Gi) - mCherry
6	OTp - DIO - hM3D(Gq) - mCherry

2.3. Virus production and purification

The procedure of virus production, transfection of permissive cells, harvesting, purification, and concentration was performed as described before (Osten, Grinevich and Cetin, 2007).

The following description of the virus production was made in the laboratory of Prof. Dr. Valery Grinevich and already published in the PhD dissertation of Dr. Ferdinand Althammer at the University of Heidelberg:

“Human embryonic kidney (HEK) 293 cells were transfected in 10x15 cm plates with the viral plasmid construct by standard calcium chloride (2M) transfection. The DNA mixture required for transfection contained the AAV expression plasmid (12.5 mg/plate), the adenovirus helper plasmid pFdelta6 (25 mg/plate) and both the AAV1 and AAV2 helper plasmids (pH21 and pRV1; 6.25 mg/plate). Transfection was performed for 48 hours, cells were scraped in phosphate-buffered saline (PBS; pH 7.4, RT), centrifuged (10 min, 800 rpm, 4°C) and resuspended in 20 mM Tris 150 mM NaCl (pH 8.4, RT). During two freeze-thawing cycles, the cells were lyzed with sodium deoxycholate (0.5% final concentration, Sigma-Aldrich) and the plasmid degraded with Benzoase (35-50 U/ml final concentration; Sigma-Aldrich) by incubation at 37°C for 1 hour. After centrifugation (15 min, 3.000 x g, 4°C) the virus containing the supernatant was loaded on a 1 ml HiTrap Heparin HP column (GE Healthcare, Chalfont St. Giles, UK) and the virus eluted under high-salt conditions (400-500 mM NaCl). Finally, the virus was concentrated and rebuffered with PBS in Amicon Ultra tubes (Millipore, Billerica, Massachusetts, USA) and filtered sterile through a 0.2 mm Acrodisc column (Pall Coorporation, East Hills, New York, USA). To prove purity and integrity of the preparation, the virus was loaded on a GelCode (Pierce Biotechnology, Rockford, Illinois, USA) and stained with sodium dodecyl sulfate (SDS)-protein gel. The genomic titer was determined by quantitative polymerase chain reaction (qPCR) using ABI 7700 cycler (Applied Biosystems, Foster City, California, USA) with primers and probes designed to WPRE” (woodchuck hepatitis virus posttranscriptional regulatory element). Adapted from (Althammer, 2017).

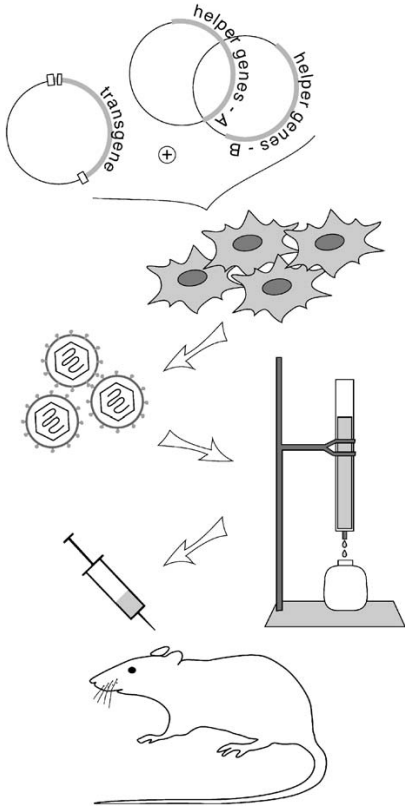

Figure 2.1 Scheme of rAAV synthesis.

Plasmids containing a transgene of interest is co-transfected with one or two helper genes into a host cell-line (HEK 239 cells). After replication of the viral genome into the host cells, new virions are produced. The viruses are either secreted to the cell medium or remain inside the transfected cells; the medium of cell lysate is collected, purified, filtrated over a chromatography column, and finally concentrated. The produced rAAV can be locally injected into a desired region of an animal central nervous system and it will infect target cells, allowing the expression of the transgene with minimal toxicity. Adapted from (Osten, Grinevich and Cetin, 2007).

2.4. Stereotactic injection of viral vectors, implantation of electrodes and optic fibers into the rat brain

All viral injections and electrode implantations have been performed as described in the methods of this studies: (Cetin *et al.*, 2006; Knobloch *et al.*, 2012). Stereotactic coordinates for targeting various brain regions are presented in the table below.

Table 2.2 Stereotactic coordinates for injection sites used for targeting of hypothalamic nuclei

Area	hemisphere	X (M-L)	Y (A-P)	Z (D-V)	Z level	dm/ vol.
SON	both	+/- 1.6	-1.4	-9	Bregma	4 / 300 nl
PVN	both	+/- 0.3	-1.8	-8	Bregma	4 / 300 nl
AN	both	+/- 1.2	-2	-8.5	Bregma	4 / 300 nl

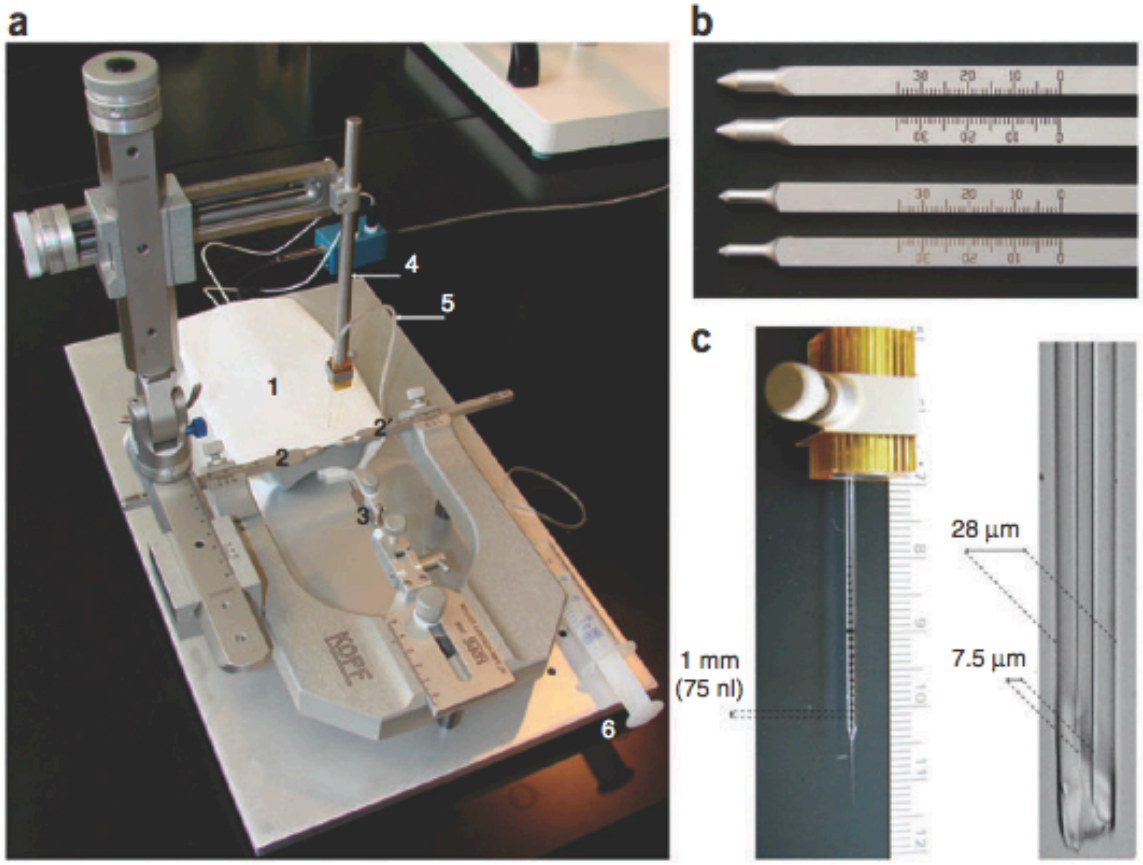

Figure 2.2 Setup for stereotaxic delivery of viral vectors into the rodent brain

*(**a**) Stereotactic device (Kopf, Germany); (**b**) Steel ear bars for use in rat (top pair) and mouse (bottom pair); (**c**) Low and high magnification image of the injection micropipette in the holder (1mm scale at right for comparison); 1 mm marks were drawn on the side of the micropipette to calibrate the injected volume: 1 mm mark = 75 nl. Adapted from* (Osten, Grinevich and Cetin, 2007).

2.4.1. Anesthesia and surgery preparation

The rat was taken by the experimenter to the surgery room 30 minutes before the anesthesia, to minimize stress for the animal. Subsequently, the animal was weighted on a scale to determine the dosage of the anesthetic. An intraperitoneal (i.p.) injection with a mixture of ketamine (65 mg/kg, b.w.) and xylazin (14 mg/kg b.w.) in 1xPBS was administered. In case of surgical procedures that lasted longer than 2 hours, the rat was anesthetized with inhalation of isoflurane (5% to induce general anesthesia and progressively lowered to 1.5-2% during the surgery and adjusted according to the animal respiration rate). The animal was ready for surgery after the absence of the withdrawal reflex to a foot pinch. The head of the animal was shaved with an electric razor and then fixed in the stereotactic apparatus. The body was positioned on a heat-controlled plate (37 °C, RWD,

China) and the head was fixed with ear bars and an incisor adaptor with a nose clamp as presented in Figure 2.3.

2.4.2. Delivery of viruses into the rat brain

The skin of the head was sterilized with 70% ethanol, cut with single incision and kept open with four surgical clips. Eye ointment (Bepanthen, Bayer, Germany) was applied to prevent the animal's eyes from drying out. The skull surface was cleaned and eventual bleeding was stopped with sterile cotton swabs. Craniotomy was performed with a pneumatic dental drill (circles of about 2 mm diameter were gently drilled).

The following description of surgical procedure is established in the laboratory of Prof. Dr. Valery Grinevich and already published in the PhD dissertation of Dr. Ferdinand Althammer at the University of Heidelberg:

"For injection of the virus 5 ml or 10 ml calibrated glass micropipettes were used. They were generated on a micropipette puller that creates a long, thin injection needle, which is cut with a scissor to get a tip opening of about 3 μm. The shaft was marked with 1 mm check marks, while 1 mark corresponds to 75 nl injection volume (see Figure 2.2 c).

The micropipette was placed into the arm of the stereotactic apparatus and connected with plastic tubing at the end. Then, a piece of parafilm with a 4-ml drop of virus was placed on a drop of PBS onto the top of the skull. The tip of the micropipette was brought into the drop of virus and suction was applied through a 20-ml syringe. The rising level was monitored through a dissecting microscope and the aspiration stopped when the desired volume was reached. Afterwards, the syringe was unplugged and the parafilm removed. Now the tip of the micropipette was moved to Bregma and the calculated x- and y- coordinates for the injection site were accessed. The micropipette was lowered until the z-coordinate was reached (the dura was penetrated with a metal needle) and the virus delivered by slowly applying pressure with the syringe. The speed and volume were controlled by visual monitoring, where the infusion rate had to be about 75 nl (1 mm across the shaft) per 10s. To avoid backflow of the virus to the surface, the micropipette was kept in this position for 5 min before being withdrawn. The injection site was cleaned with PBS and the skin sutured. Until full recovery, the rat was kept on a temperature-controlled heat blanket, and then placed back into the home cage with *ad libitum* access to food and water." Adapted from (Althammer, 2017).

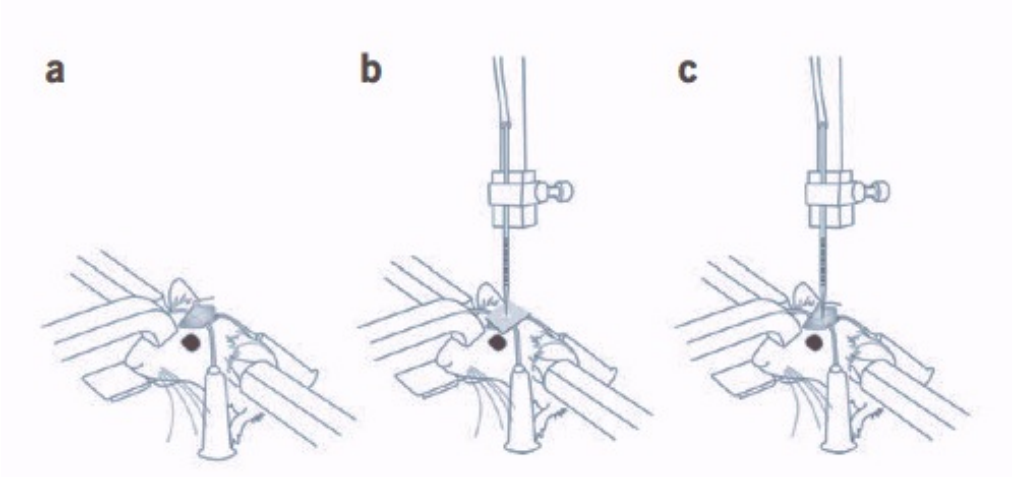

Figure 2.3 Surgery and delivery of the virus

*(**a**) The surgical wound is kept open by short needles with blunted tips bent to form small hooks. (**b**) After the craniotomy is drilled, virus (a 4-μl drop on parafilm positioned atop of the skull) is aspirated into the micropipette by suction with a 20-ml syringe attached by a thin tubing; aspiration of the virus in the shaft of the micropipette is monitored with a dissecting microscope. (**c**) After the micropipette is positioned in the brain parenchyma at the desired x, y and z coordinates, the virus is injected by slow pressure with a hand-held syringe. The speed and volume of the injection is monitored as the top level of the virus solution moves across the calibration marks on the micropipette, with 1 mm corresponding to 75 nl of injected volume. Adapted from* (Cetin *et al.*, 2006).

2.4.3. Implantation of electrodes and optic fibers[1]

The first part of the surgical procedure for chronic implantation of recording electrodes (tetrodes or silicon probes) or optic fibers into the rat brain is identical to the one described in the previous paragraph for delivery of virus through a micropipette. Once the skull surface has been cleaned and the craniotomy performed, the implanted device is placed at the desired x- and y- coordinates and slowly propelled (500 μm/minute) down to the target depth. After the device has been implanted in the correct position four steel screws (Knupfer, Germany) are positioned symmetrically onto the skull surface; subsequently, the electrode and the screws are fixed to the skull by applying dental glue and dental cement (Paladur, Heraeus Kulzer, Germany). In the case of the electrodes, a protective cap is positioned around the implantation site to prevent the animal from damaging the implant while moving or scratching itself.

[1] All opto-electrode implantations were done by or under the supervision of dr. Yan Tang.

The silicon probes used for PVN *in-vivo* recordings were of the type A1x32-Poly3-10mm-50-177-OH32LP_21mm (NeuroNexus, U.S.A.), and the tetrodes were made with 0.0005 inches tungsten wires (Stablohm 675, California Fine Wire Company, U.S.A.). Assembled tetrodes were gold plated and impedance of each channel was measured between 250 and 350 kOhm.

2.5. Single units recording *in vivo*

2.5.1. Spike sorting

To discriminate action potentials recorded from different neurons, spike sorting based on spike waveform differences was performed. “Spike sorting was done manually in Plexon Offline Sorter 4.0 (Plexon, Inc., TX, USA), with tetrodes mode. The raw data were filtered at 250 Hz with a butterworth high-pass filter, and waveform detection thresholds were placed at -0.5-0.8% of ADC range (or -0.32 ~ -0.51 mV), depending on the signal-to-noise ratio. Magnocellular neurons have spikes with a width at half amplitude of about 0.5 ms, an absolute refractory period of about 2.5 ms and a long relative refractory period reflecting a prominent hyperpolarizing afterpotential (Maícas-Royo, Leng and MacGregor, 2018). Therefore, the sample length in waveform detection was set to 1.4 ms (400 µs pre-threshold period, at the 30 kHz sampling rate, a single waveform consists of 42 data points, and in the tetrodes waveform, each unit detected 168 data points), and dead time was set to 1.2 ms. Next, the detected waveforms were aligned at the valley point, when extracellular spikes were depolarized at their maximum, and Principle Component Analysis (PCA) and Slice features of waveform were plotted and projected into 3D space for visual separation of clusters into presumptive single-units. The timestamp feature was used to exclude mechanical noise recorded at same time across 4 channels among the tetrodes. In different recording sessions (e.g., open field and social interaction), we analyzed whether the features of tetrode waveforms remain consistent with the 3D plot results. After clustering, units with a minimum inter-event interval exceeding 2500 µs were accepted as single hypothalamic neurons. Units displaying minimum inter-event intervals between 1200-2500 µs were recognized as arising from multiple neurons and were excluded from the statistics of the study.” Method adapted from (Tang *et al.*, 2016).

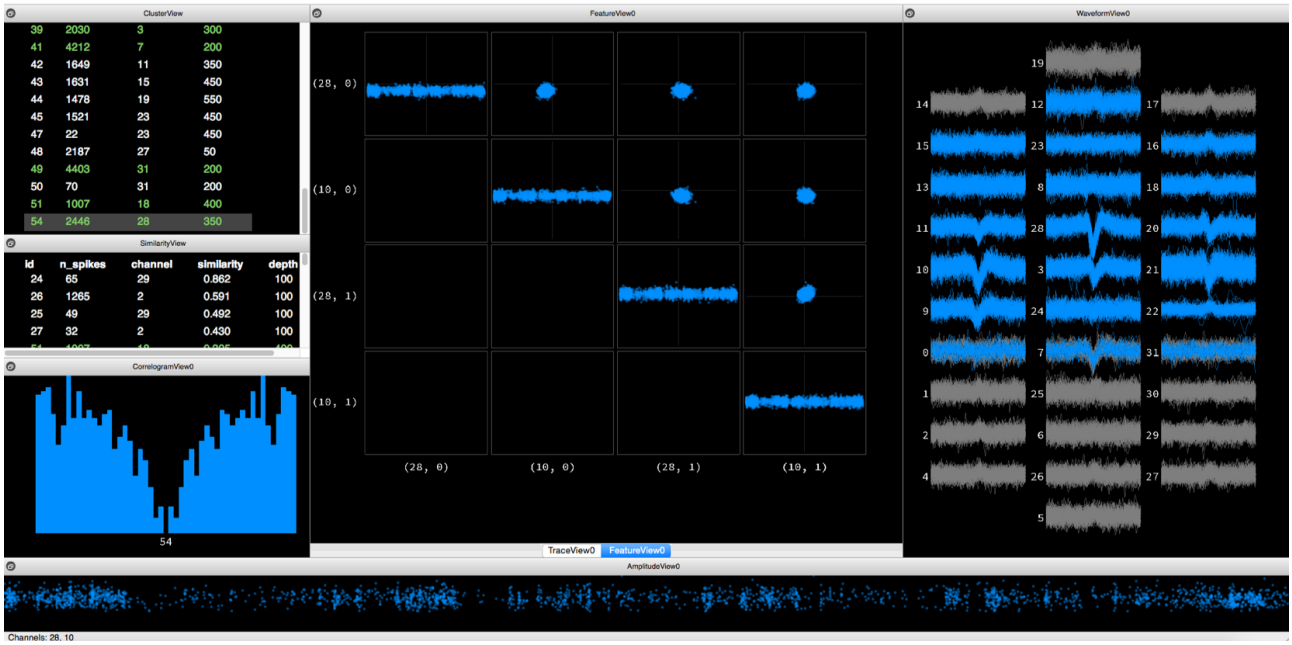

Figure 2.4 Spike sorting pipeline with Phy.

Screenshot from the user interface of the spike sorting algorithm klusta-Phy. The spike sorting algorithm was used to discriminate action potentials recorded from different neurons. Each neuron has a characteristic 'signature' in terms of the shape of the waveform (graphic of the membrane potential as a function of time) that is unique for each cell. The algorithm is able to differentiate reliably tens of simultaneously recorded neurons based on the difference of their waveforms. The details of the algorithm are published and available online (Rossant et al., 2015).

2.5.2. Optogenetic identification of individual oxytocin neurons *in vivo*

Recording extracellular action potential from a genetically defined population of neurons – as the oxytocin neuron population – is possible thanks to the transduction of the light-sensitive ion-channel channelrhodopsin2 (ChR2) into those cells via viral vectors. Once ChR2 is expressed in the cell population of interest, an opto-probe consisting of an optic fiber cannula connected to a recording electrode probe is lowered into the region of interest into the rat brain. Blue light pulses (wavelength λ = 473 nm) generated from a laser (power = 10 mW measured output, DreamLasers) are delivered through the optic fiber into the brain region where oxytocin neurons are located; simultaneously, electrical potentials from the extracellular medium are recorded by the electrodes. After sorting the action potential (spikes) into putative individual neurons according to the shape of their waveforms, peri-stimulus time histograms (PSTHs) of spike times of recorded neurons are aligned to the onset of blue light pulses. Only those cells which are expressing ChR2, *i.e.* only oxytocin

neurons, will show a clear and time-locked correlation between spike times and blue light onset.

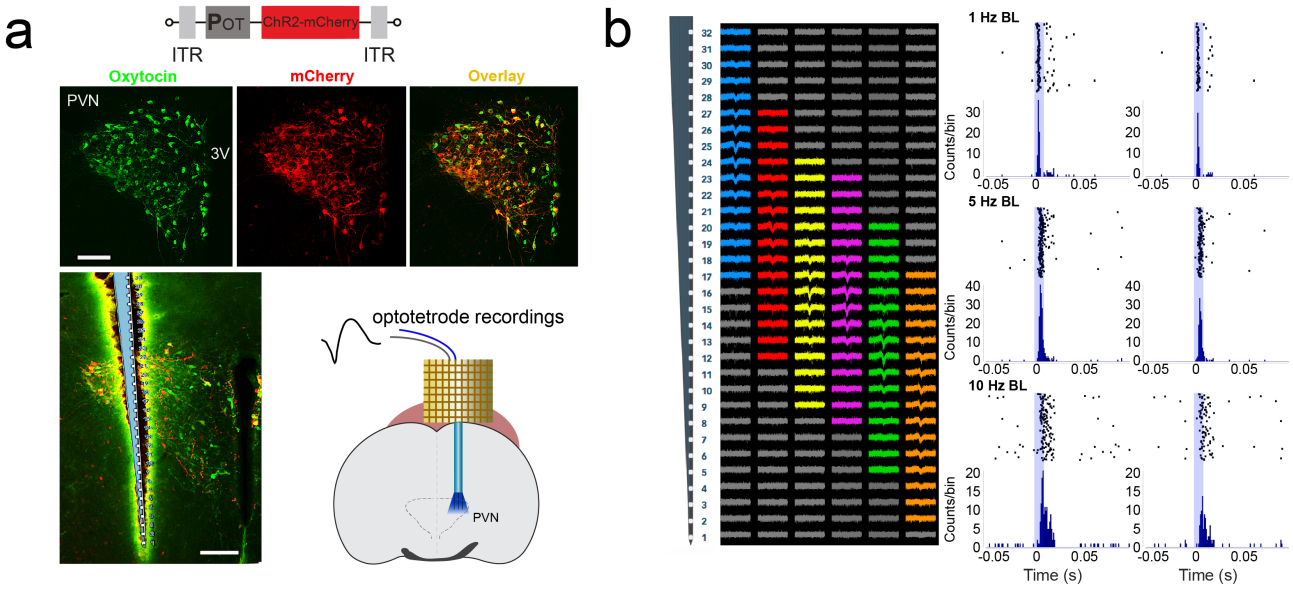

Figure 2.5 In-vivo optogenetic identification of oxytocin neurons.

*(**a**) Recombinant adeno-associated virus OTp-ChR2-mCherry is injected into the PVN of hypothalamus to transduce the expression of Channelrhodopsin2 in oxytocin neurons.*

*(**b**) Silicon probe (NeuroNexus) with 32-channel single shank were used in acute (anesthetized) recording of oxytocin neurons. Sorted units and their location in the channels map are visualized with Phy-GUI (klusta, Python). PSTHs indicate putative oxytocin neurons responses to blue-light pulses at 1 Hz, 5 Hz, and 10 Hz frequency of stimulation.*

I used a strict criterion to differentiate ChR2-expressing oxytocin versus non-oxytocin neurons based on their response to blue-light pulses.

Once an oxytocin neuron is identified among the recorded units, the shape of action potential (waveform) is saved by the spike sorting algorithm and used later on to discriminate oxytocin cells among the other detected neurons.

2.6. Fiber photometry

Fiber photometry is a technique that allows to record the activity of a cell specific neuronal population using genetically encoded calcium indicators (GECIs) and a single multimode optical fiber (Gunaydin *et al.*, 2014).

2.6.1. Genetically encoded calcium indicators

The intracellular concentration of free calcium ions [Ca^{2+}] is a good indicator of neuronal activity, therefore fluorescent calcium reporter proteins have been designed to measure real-time activity of large populations of neurons *in vitro* and *in vivo* (Tian *et al.*, 2009) in a non-invasive manner. Among those calcium reporter proteins, GCaMP (Nakai, Ohkura and Imoto, 2001), has become a popular tool in the neuroscience community. All the proteins from the GCaMP family consist of a circular permutated green fluorescent protein (cpGFP), the calcium-binding protein calmodulin (CaM) and CaM-interacting M13 peptide. The GCaMP has low fluorescent level in its ground state, but in presence of free calcium ions, which bind to the CaM-M13 complex, a conformational change of the protein causes a fast and transient increase in brightness that can be detected through imaging.

The combination of this technology with viral vectors allows the experimenter to selectively transduce the expression of GCaMP in genetically defined cell populations in living organisms. With this technique, imaging from a cell-specific neuronal population, also in deep regions of a mammalian brain, such as the oxytocin neurons population in the PVN of mice and rats, has become accessible.

2.6.2. Fiber photometry recording

In fiber photometry recording the excitation light and the emitted fluorescent signal are delivered and collected by a single multimode optic fiber. The optic fiber is connected through a patch cord and coupled to a laser or LED source and a photodetector via a fiber splitter. The emission light (wavelength) is delivered to the region of interest in the brain through the implanted optic fiber and the photons emitted by the fluorescent signal are reflected back to the photodetector.

The major tradeoff of fiber photometry systems is reducing the physical size of the implanted fiber and the intensity of the injected light to avoid damage in the tissue and photobleaching, while still keeping a reasonably high signal-to-noise ratio (S/N) (Pashaie and Falk, 2013). To address this compromise, the emitted light pulses are modulated at high frequency and the collected light is amplified by a photo-multiplier to elevate the instantaneous S/N without sacrificing the temporal resolution. In our experiments, we employed a fiber optic (ThorLabs) with 400 μm silica core that allowed optimal detection of PVN oxytocin neurons calcium signal without causing sensible damages to brain tissues. During recording sessions all the light in the room were turned off to minimize ambient noise.

2.7. Behavioral tests

Behavioral tests were conducted in an arena - a box made of a material non-absorbent to odors, with dimensions 60x60x60 cm - under dim light condition (< 20 lux; lux-meter SO 200K, Sauter, Germany). On the day before the test, the experimental rat was exposed to the arena for 15 min for habituation. The arena was cleaned with 70% ethanol after each session to eliminate residual odors. Experimental and stimuli rats were housed in separate cages and had not previous encountered each other before the social interaction tests. In all the experiments in which the same rat was exposed to social interaction tests more than once, it was done on separate days, each time with a different social stimulus rat so that the experimental paradigm always represented interaction with a novel, unfamiliar conspecific. The three type of behavioral tests that were used throughout all experiments were open field tests, free social interaction tests, and chambered social interaction tests and were performed as follows:

Open field (OF) test:

The experimental rat was placed in a corner of the arena and was allowed to freely explore the environment. These tests served as a "baseline" for social interaction tests.

Free social interaction (FSI) test:

The experimental and the stimulus rats were placed in opposite corners of the arena at the same time and were allowed to freely interact with each other and/or explore the environment.

Chambered social interaction (CSI) test:

The setup for this test was adapted from (Netser *et al.*, 2017). Two plexiglas transparent meshes (dimensions 20x30x1 cm) provided with three opening/holes (dimensions 15 x 0.75 cm) were placed in two opposite corners of the arena. The mesh separated a little triangular area (14 x 14 x 20 cm, corresponding to ~3% of the total area of the arena) to the rest of the arena (central compartment). The experimental rat was placed in the central compartment while the stimulus rat was placed in one of the two little compartments. The two rats were able to see, hear, and smell each other through the openings, but they were not able to touch one another.

2.7.1. Estrous cycle phases of female rats

Starting from 14 days prior to behavioral tests, cytological vaginal smears were collected to monitor ovarian cycle. The characterization of each phase of the cycle is determined based

on the proportion of cells observed in the vaginal smear among the cell types: epithelial cells, cornified cells, and leukocytes (Marcondes, Bianchi and Tanno, 2005). The Rats in metestrus, proestrus, and estrus phases were excluded from experiments and reintroduced once they reached diestrus.

2.8. Intra-cardiac perfusion

The rat was put into an exicator containing isoflurane until the breathing stopped. Then it was immediately fixed on a board and the thorax was exposed by using forceps and scissors. The thoracic cage was cut to access the heart, which was still beating. It was taken out of the pericardium to place the perfusion needle into the left ventricle. The right atrium was opened with small scissors and the peristaltic pump of the perfusion setup was turned on. The circulation was flushed 3-5 min with phosphate-buffered saline (PBS) containing heparin (1.3 ml heparin sodium in 200 ml 1xPBS) until the whole blood volume was washed out of the body. Afterwards, the tubing with PBS was closed and the one containing 4% paraformaldehyde (PFA) opened and the fixation performed for 20 min. As a next step, the brain of the rat was extracted and post-fixed overnight at 4°C in a mixture of 15 ml PFA in 35 ml PBS with gentle-agitation. After post-fixation, the brain was kept in PBS on 4°C in the cold room before sectioning.

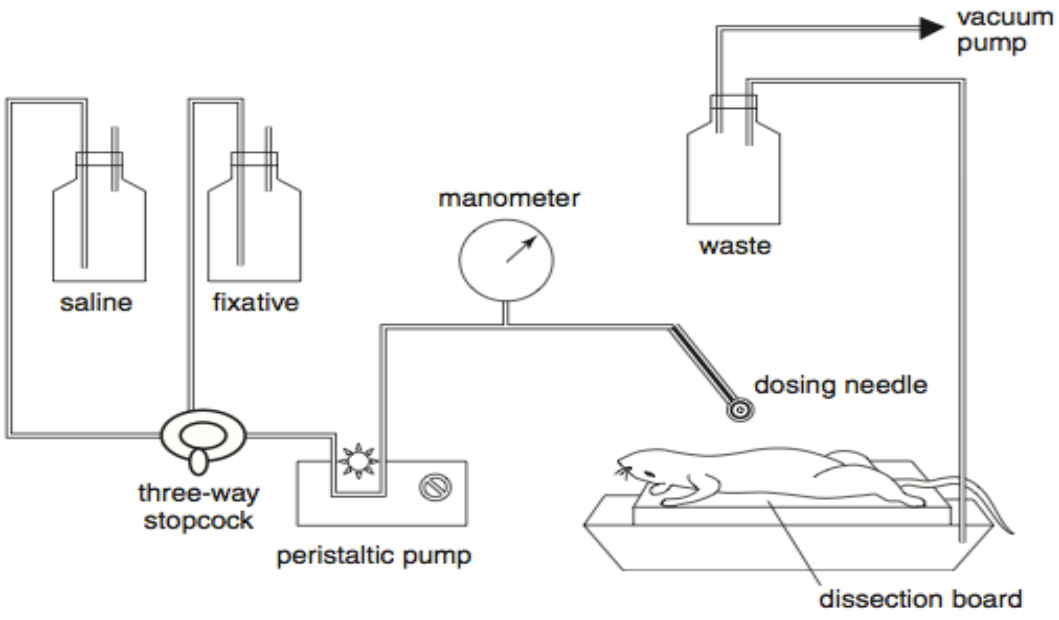

Figure 2.6 Perfusion setup

Adapted from: http://www.currentprotocols.com/protocol/tx1603

2.9. Slicing of the brain

The brain was cut in 3 coronal blocks with the use of a glass matrix. The middle part of the brain, containing the hypothalamus and amygdala was sectioned using a vibratome (Leica VT1000S, Germany) to obtain coronal slices of 50 µm thickness. Sections were transferred into well plates with cold PBS and stored at 4°C until the processing.

2.10. Immunohistochemistry

50-µm vibratome coronal sections containing the PVN and the SON were cut and collected. Immunohistochemistry was performed on free-floating sections with the following antibodies: anti-OT (PS38, 1:2000; mouse; kindly provided by Harold Gainer), anti-Ds-Red (1:1000; rabbit; Clontech), anti-mCherry (1:1000, chicken, Abcam), anti c-Fos (1:500, rabbit, Cell Signaling), anti-Fluorogold (1:1000, guinea pig, Protos Biotech). The signals were visualized with the following secondary antibodies, CY3-conjugated or CY5-conjugate (Jackson Immuno-Research Laboratories) or Alexa 350 and 594 (Invitrogen). All secondary antibodies were diluted 1:500.

2.10.1. Immunofluorescent staining

The protocol for immunofluorescent staining of fixed brain sections comprised the following steps:

1. Blocking step: pre-incubation of sections in buffer (1% Triton in 1xPBS, 4 slices for each ml of buffer) with 5% of NGS (normal goat serum). 2 hours at room temperature with gentle agitation.
2. Primary step: incubation of sections in buffer (1% Triton in 1xPBS) with primary antibodies. 24-48 hours at 4°C (cold room) with gentle agitation.
3. First washing step: washing of the sections from primary antibodies in 1xPBS. 4 times per 10 min with gentle agitation.
4. Secondary step: incubation of sections in buffer (1% Triton in 1xPBS) with secondary antibodies. 2 hours at room temperature, in dark, and with gentle agitation.
5. Second washing step: washing of the sections from secondary antibodies in 1xPBS. 4 times per 10 min with gentle agitation.
6. Mounting step: sections were mounted on Superfrost Plus (Thermo scientific) microscope glass slides (4 sections per slide), dried out, and covered with glass slips (24x50 mm, Roth).

2.10.2. Fluorogold treatment and visualization

To discriminate between magno- and parvocellular oxytocin neurons, rats received a single injection of Fluorogold (Santa Cruz Biotechnology, Dallas, 15 mg/kg bw i.p.) 7 days before the perfusion. Brain sections were stained with a primary antibody for Fluorogold (guinea pig anti-FG, dilution 1:1000, Protos Biotech Corp, New York) and Fluorogold immunosignal was visualized by secondary antibodies conjugated with CY3 (Goat anti-rabbit, dilution 1:500, Jackson Immuno-Research, Newmarket Suffolk, UK). The colocalization of Fluorogold, oxytocin, and c-Fos signals in the PVN were manually quantified on high-resolution confocal images (N = 8 animals; 6 sections/brain).

2.11. Microscopic imaging of immuno-stained sections

High-quality images of immune-stained tissue sections were acquired on a Leica TCS SP5 (DKFZ Light Microscopy Facility) confocal laser-scanning microscope. Digitized images were analyzed using Fiji (NIMH, Bethesda, MD, USA) and Adobe Photoshop CS5 (Adobe, Mountain View, CA).

2.12. Mathematical model for estimation of oxytocin release[2]

The oxytocin secretion model (Maícas-Royo, Leng and MacGregor, 2018), that simulates stimulus-secretion coupling in oxytocin neurons, is a continuous approximation of the stochastic release process from all neuronal compartments. In other words, it is a mathematical model that takes as inputs a spike train (sequence of time of action potentials) of an oxytocin neuron and gives as output an estimation of the amount of peptide released from that cell during the same period of time. The model is based on extensive studies on activity-dependent hormone secretion from magnocellular neurosecretory cells (Maícas Royo *et al.*, 2016) and it matches experimental data closely. Since the relationship between spike time intervals (time between two consecutive action potentials) and peptide secretion probability is highly non-linear, different spike trains – even with the same number of spikes – can result in very different amount of estimated peptide secreted. Typically, sequences of action potentials with very little intervals between them (spike bursts) will trigger high secretion rates; on the contrary, regular firing with long intervals between consecutive spikes will lead to low peptide secretion.

[2] Calculation of predicted oxytocin release was done by Jorge Maicas Royo and Prof. Gareth Leng based of the oxytocin neurons spike trains data collected in the present work.

I used this model to make a quantitative estimation of the amount of oxytocin released from all neuronal compartments, including axons, collaterals, and dendrites, of the oxytocin cells recorded during free exploration in the open field arena, during chambered and free social interactions, based on the spike trains of those neurons. With this method, it is possible to evaluate the changes in oxytocin release upon different stimuli or behavioral states of the animal at the single cell level.

2.12.1. Model implementation

In the model, when spikes invade the secretory terminals, exocytosis occurs in response to fast rising Ca^{2+} concentrations (*e*). At higher frequencies, the spikes broaden, producing a larger increase of *e*. The rate of secretion is modeled as the product of: *e* raised to the power of φ (which accounts for the cooperativeness of the Ca^{2+} activation), of the pool of releasable oxytocin *p*, and a secretion scaling factor α, and is calculated as:

$$s = e^{\varphi} \cdot \alpha \cdot p$$

where $\varphi = 2$, $\alpha = 0.003$ pg/s.

The non-linear dependence of the secretion rate gives high secretion probability upon short spike intervals. To infer oxytocin secretion arising from the spike trains observed in the present study, the recorded event timings were used to drive the secretion model described fully elsewhere (Maícas-Royo, Leng and MacGregor, 2018). The published model is scaled to quantitatively match secretion from the pituitary nerve terminals of a single oxytocin neuron. The scaling factor α cannot be used for absolute quantitative estimates of release within the brain, but the relative efficacy of two firing patterns can be compared using the model, as α is eliminated in the ratio.

2.13. Statistical analysis

Statistical analysis was performed applying the appropriate test or method in each experimental paradigm. Student's two-tailed unpaired *t*-tests were used to compare average values in two conditions when the data satisfied assumptions of normality. One-way ANOVA, followed by multiple comparison *post-hoc* Tukey's test, was used to compare averages in three or more conditions. Two-way ANOVA, followed by multiple comparison *post-hoc* Tukey's test, was used to analyze behavioral data with repeated measures and CNO or saline treatment (time x treatment). Wilcoxon signed-rank test was used to compare the variation of spike frequencies measured for the same neuron in different conditions.

Differences were considered significant for $p < 0.05$. Asterisks were used to indicate the significance level: * $0.01 \leq p < 0.05$, ** $0.001 \leq p < 0.01$, *** $p < 0.001$.

Classical statistical tests were performed using SigmaPlot 11 (Systat, USA). Statistical analyses of neuronal spike trains and local field potentials, such as peristimulus time histograms (PSTHs), auto- and cross-correlation, spikes burst analysis, power spectrum density, and phase-locking were performed using custom MATLAB scripts.

Chapter 3: Results

3. Results

3.1. *In vivo* recording of individual oxytocin neurons in the PVN

Measuring the activity (*i.e.* action potentials) of cell type specific neuronal population *in vivo* is a key step to understand their functionality. To record extracellular action potentials from single oxytocin neurons, rats were injected with a recombinant adeno associated virus (OTp-ChR2-mCherry), in the PVN to transduce the expression of the light-sensitive ion channel channelrhodopsin2 (ChR2) and expression of the fluorescent marker mCherry under the control of the oxytocin promoter. After three weeks of viral expression, rats were implanted in the PVN with custom-made tetrodes or silicon probes (NeuroNexus) combined with an optic fiber (∅ 200 μm, Thorlabs). Once the electrodes were propelled at the target depth, field potentials and extracellular action potentials were recorded from PVN neurons while pulses of blue light where delivered in the same area. Among the 90 PVN single units recorded, 15 were strictly identified as oxytocin neurons by their response to blue light pulses. The shape of the action potential waveform of each recorded neurons was saved and used to discriminate oxytocin cells from other non-oxytocin PVN neurons during the experiment. The identification procedure was repeated also at the end of each recording session as an additional control.

This procedure was applied in two different types of experiments: in awake freely moving experiments and in anaesthetized experiments.

3.2. Awake freely moving recordings

One of the main goals of the project was to measure the electrical activity of individual oxytocin neurons during freely moving social interaction in female rats. Two batteries of tests were performed in the context of this experiment:

1. Open field and free social interaction;
2. Open field, chambered social interaction, and free social interaction.

3.2.1. Open field and free social interaction

In the open field arena, i.e. when the rat was alone, the pattern of spiking of oxytocin neurons was characterized by low rate of tonic firing with a low index of dispersion (< 1) and a distribution of inter-spike intervals consistent with random spike generation subjected to a

prolonged relative refractory period. By contrast, the same oxytocin neurons showed increased activity during episodes of social interaction with an unfamiliar conspecific. Specifically, during those episodes the cells fired at a higher rate (average increase 1.5 ± 0.4 spikes/s, p = 0.001, n = 15) and more irregularly; the index of dispersion was significantly higher (FSI, 3.2 ± 0.4; CSI, 1.3 ± 0.3, p = 0.006 vs FSI; open-field, 0.9 ± 0.2, p = 0.004 vs FSI, n = 15), reflecting the increased occurrence of spikes clusters. In anesthetized rats, spike clustering and spike synchronicity is not seen in most conditions where oxytocin cells are activated (Brown *et al.*, 2013), but it is seen in lactating rats during suckling (Brown, Fontanaud and Moos, 2000).

Cross-correlation analysis was performed on pairs of simultaneously recorded oxytocin neurons revealed an increased spike synchronicity during social interaction compared to open field (average pairwise correlation: open field, 0.10 ± 0.04; FSI 0.40 ± 0.08, p = 0.001, number of cell pairs = 17).

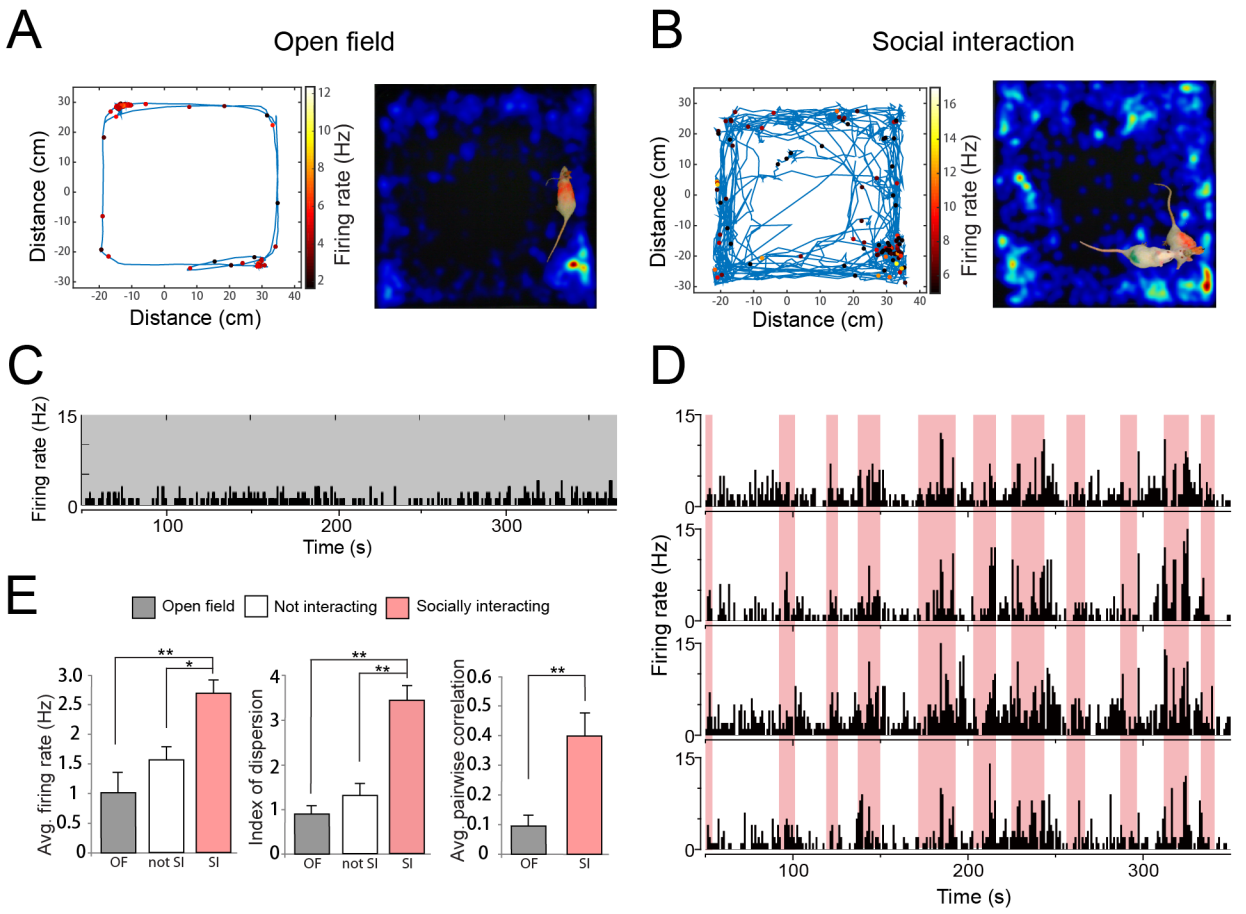

Figure 3.1 Recording of PVN oxytocin neurons during social interaction

*Example of baseline recording from a rat alone in the open field arena (**A**) and during free social interaction (**B**); animal movement path (blue line), location of prominent oxytocin cell activity (colored dots), heatmap of time spent by the rat in different locations.*
*(**C**) Example firing rate (1-s time bins) of a single identified oxytocin cell recorded during open field (baseline) test.*
*(**D**) Example firing rate of four identified oxytocin neurons recorded simultaneously during FSI. Red bars indicate periods of social interaction.*
*(**E**) Average firing rate of 15 oxytocin neurons from five rats in open field (OF), not socially interacting (not SI), and social interacting (SI). Average index of dispersion on 1-s time bins of 15 oxytocin cells. Average pairwise Pearson correlation of spiking activity (1-s time bins) of oxytocin neurons' pairs recorded in the same rat in OF and SI. All data show average + SEM.*

In addition to neuronal spikes, we also recorded local field potentials in the PVN in the open field and during social interaction. Immediately after the introduction of the conspecific stimulus in the arena and for the whole duration of social interactions, a significant increase of the oscillatory power in the theta (5-10 Hz) frequency band was registered. Phase-lock analysis revealed a correlation between the spiking activity of oxytocin neurons and theta oscillations during free social interaction, but not in the open field arena, when the animal was alone.

3.2.2. Dissection of sensory response of oxytocin neurons

To dissect sensory modalities which preferentially activate oxytocin neurons during free social interaction, we classified rat social behaviors into '*sniffing*', '*head-to-head*', '*mounting*', '*being mounted*', or '*chasing*', and constructed peristimulus time histograms (PSTH) of spiking activity before, during, and after the onset of each sequence. *Mounting* and *being mounted* induced the highest increase in firing rates of oxytocin neurons (mounting: average increase 1.7 ± 0.4 spikes/s, $p = 0.036$; being mounted: average increase 1.9 ± 0.4 spikes/s, $p = 0.024$), while, *sniffing*, *chasing*, and *head-to-head* events induced little or no changes (see Fig. 3.2). This is one evidence that suggests that somatosensory component of social interaction (*i.e.* 'social touch') plays an important role in activating oxytocin neurons.

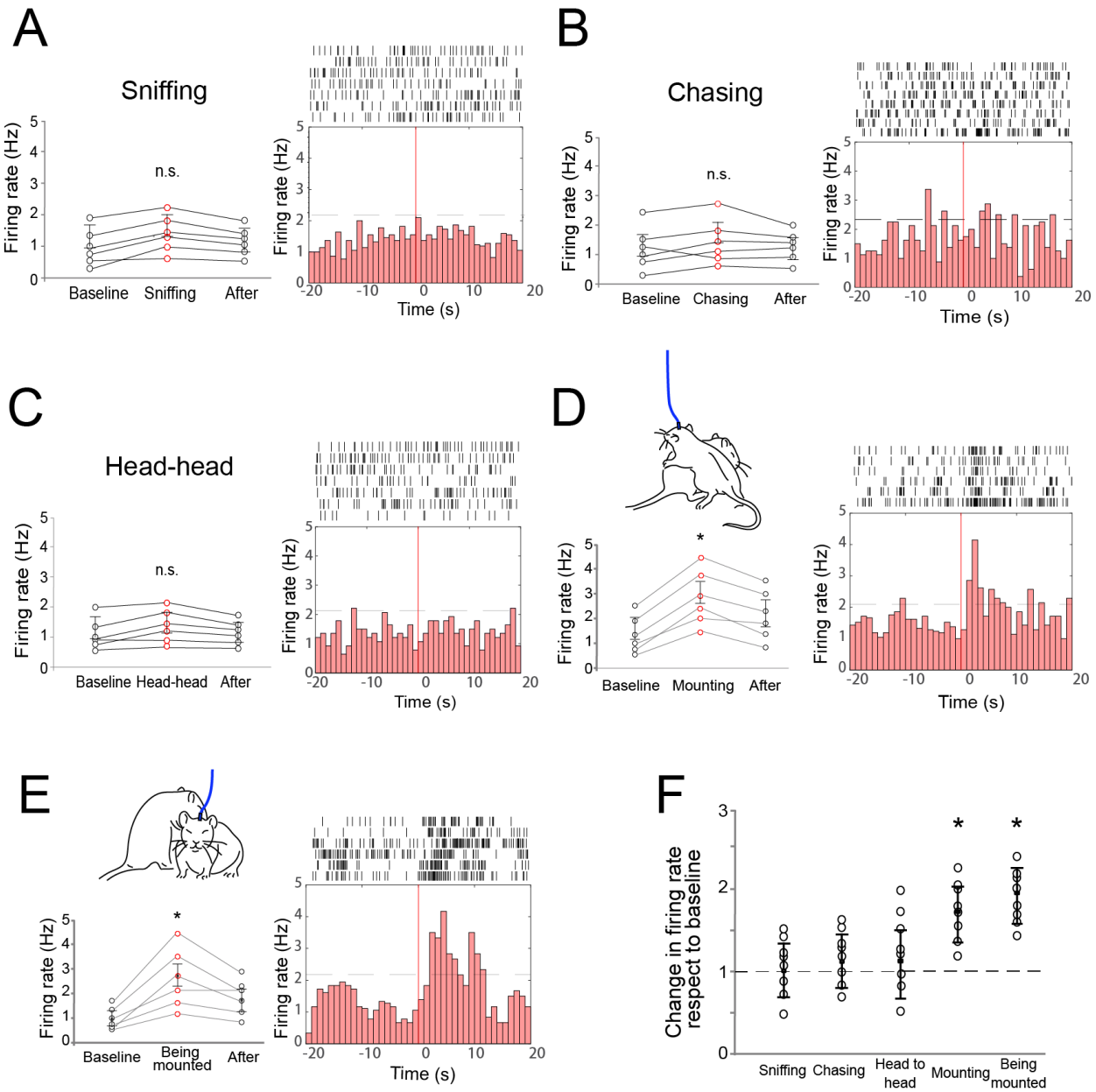

Figure 3.2 Dissection of sensory response of oxytocin neurons

*Representative spike raster plots, averaged response, and PSTH of oxytocin cell spiking activity aligned to five different social behaviors: sniffing (**A**), chasing (**B**), head-head (**C**), mounting (**D**), and being mounted (**E**). (**F**) Comparison of average change (10 s after) in firing rate of oxytocin neurons respect to baseline (10 s before) for each of the five social behaviors analyzed. All data show average ± SEM.*

Ultrasound vocalizations were recorded during the whole experiment with an ambient microphone. When the rat was alone in the open field arena, very few vocalizations were detected (0.3 ± 0.1 vocalizations/min); in contrast, during free social interaction, vocalizations were very numerous (42 ± 20 vocalizations/min). The analysis of the sound

spectrogram revealed that most vocalizations had a frequency in between 40 and 90 kHz, which is a frequency band known to be related to social communication in rats (Portfors, 2007). However, PSTH analysis of oxytocin neurons spikes aligned to vocalization times found no time-locked (up to 5 seconds range) correlation between the two events. Therefore, we concluded that there is no strict relation between oxytocin neurons activity and ultrasound vocalizations.

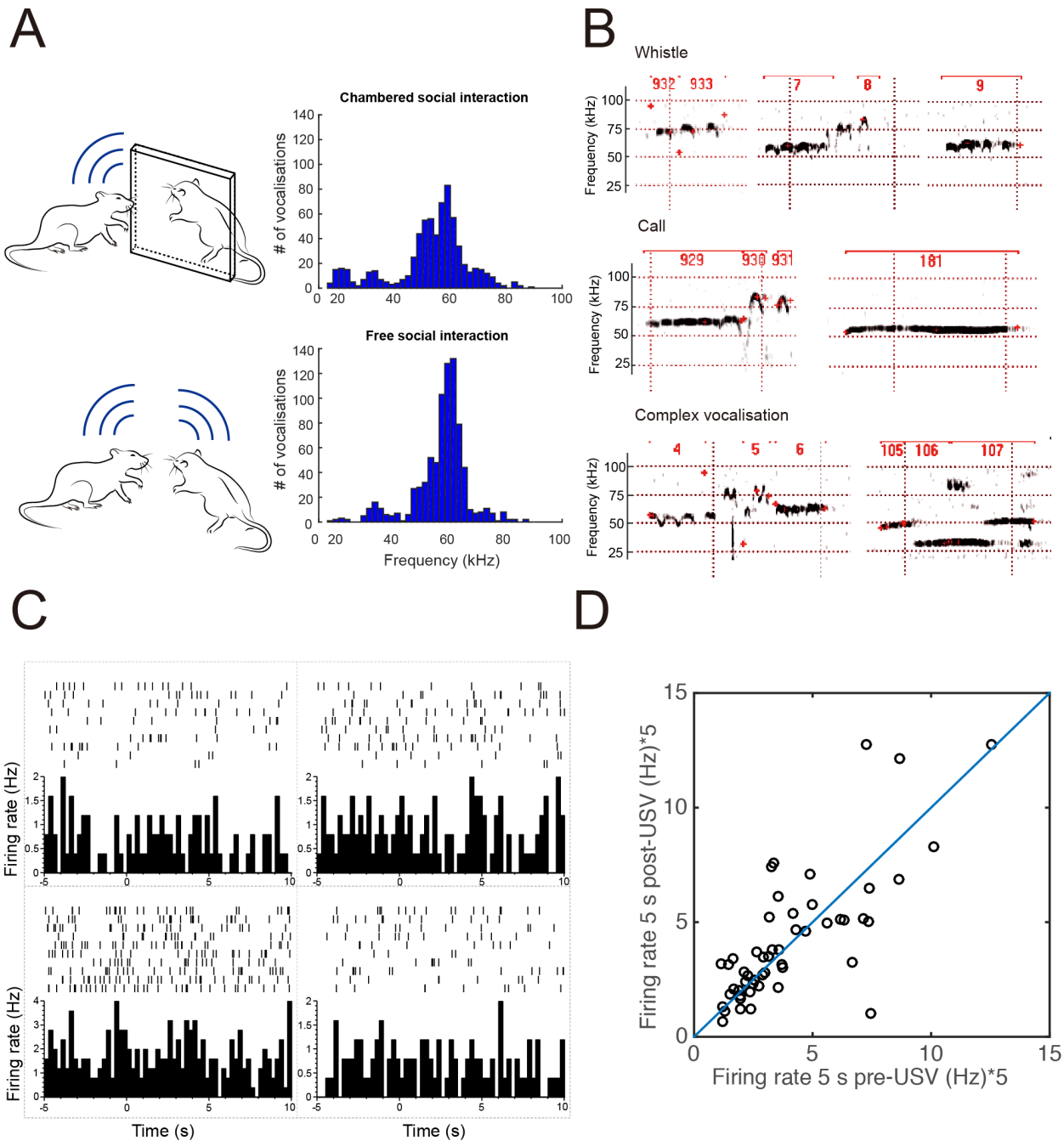

Figure 3.3 Ultra Sound Vocalizations (USVs) of rats during social interaction.

*(**A**) Histograms of USVs peak frequency distribution during CSI (top) and FSI (bottom). (**B**) Examples of sound spectrograms showing USVs events classified as whistles, calls, or*

*complex vocalizations. (**C**) PSTHs of oxytocin neurons spiking activity aligned to USVs show no significant time-locked correlation between them. (**D**) Firing rate of oxytocin neurons 5 s before USV events versus 5 s after USV events showing no significant correlation (p = 0.24, Wilcoxon signed-rank test).*

3.2.3. Chambered social interaction

As described in paragraphs 3.2.1 and 3.2.2, oxytocin neurons showed a clear increase in firing rate and synchronicity level during free social interaction, especially during those moments in which the animals were touching each other (*mounting* or *being mounted*). As a second step, we wanted to understand whether the sensory component of the social contacts was necessary for activating the neurons, hence we recorded oxytocin cells activity during a chambered social interaction (CSI). In this context, experimental and stimulus rats were separated by a mesh (a plexiglass wall with small openings) which allowed the animals to see, sniff, and hear each other, but not to touch each other. The spiking activities of oxytocin neurons in the open field arena, during a chambered social interaction, and during a free social interaction were compared. During the CSI test, although the experimental rat spent on average (32 $\pm$ 6) % of the time investigating the chamber where the stimulus rat was located, oxytocin neurons showed only a very little change in spiking activity compared to the baseline (average change 0.4 $\pm$ 0.3 spikes/s, n = 15, not significant). After the CSI test, the wall separating the rats was removed to allow free social interaction; recorded oxytocin neurons showed increased firing rate and synchronicity during social contacts periods, as in the previous experiment (average firing rate change 1.6 $\pm$ 0.4 spikes/s, p = 0.001; average index of dispersion change 2.3 $\pm$ 0.4, p = 0.004, n =15). Ultrasonic vocalizations in CSI and FSI were comparable in number and emission frequency, but in none of the case they were strictly correlated to oxytocin neurons firing activity.

3.2.4. Estimated oxytocin release during social interaction

In previous paragraphs, I showed that free social interactions cause an increase of the spiking activity of PVN oxytocin neurons and a re-organization of the spike distribution (measured by the index of dispersion) with the appearance of “spike clusters”.

I employed an activity (spike) dependent model of oxytocin secretion (Maícas-Royo, Leng and MacGregor, 2018) to estimate the peptide release probability given the recorded spike trains of oxytocin neurons (see Methods section for details). This model captures the non-

linear enhancement of peptide release upon spike clusters: short spike intervals give high secretion probability.

Based on the firing activity of oxytocin neurons recorded in the freely moving experiments, we calculated the estimated average amount of oxytocin released from all neuronal compartments during the open field test, the chambered social interaction test, and the free social interaction test. During free social interaction, the predicted oxytocin secretion was three times higher than during chambered social interaction or open field test (FSI vs OF: p = 0.002; FSI vs CSI p = 0.003 respectively; no significant difference between CSI and OF p = 0.28, n = 15).

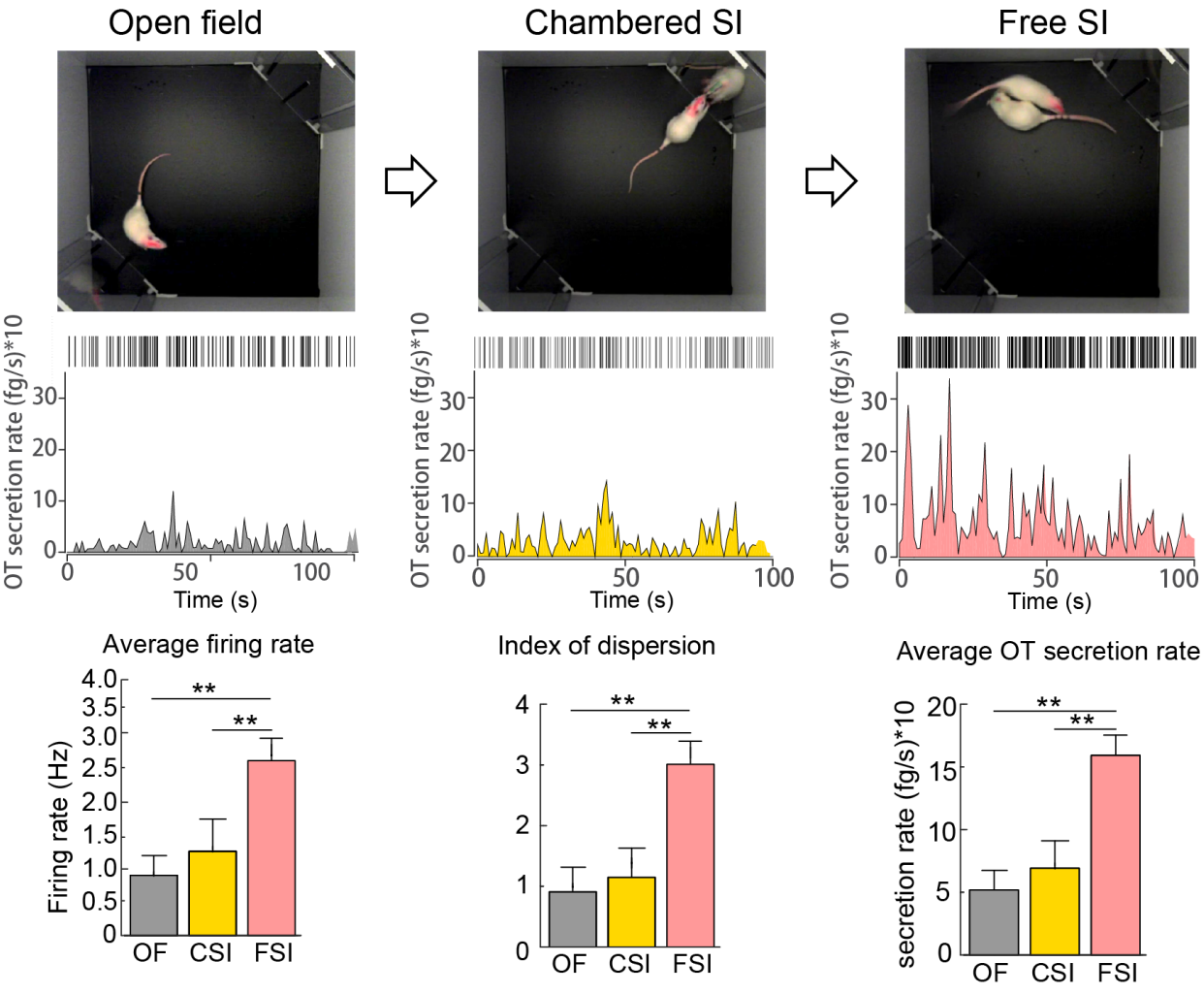

Figure 3.4 Estimated oxytocin secretion in different conditions

Top: experimental rats were placed either alone (open field, OF), with a stimulus rat but separated by a barrier (chambered social interaction, CSI), or together with a stimulus rat (free social interaction, FSI). Middle (black bars): representative spike rasters plots for each condition. Bottom: predicted secretion rate for a representative cell in each condition.

Left: average firing rate of oxytocin neurons in each of the three conditions (OF, CSI, and FSI). Middle: average index of dispersion of oxytocin neurons. Right: average predicted oxytocin secretion rate. All data show average + SEM.

3.3. Anaesthetized recordings

Somatosensory component of social interaction is related to increase of oxytocin neurons activity. Is the 'touch' itself sufficient to trigger an increase in spiking activity of PVN oxytocin neurons? To answer this question, I recorded extracellular single-units PVN neurons activity during controlled tactile stimulations using compressed air delivery ('airpuffs') while the animals were lightly anaesthetized. Once again, oxytocin neurons were identified among PVN cells by optogenetic tagging prior to the experiment.

3.3.1. Application of 'airpuffs'

Airpuffs from a pressured air can (Toolcraft 20793T 400 ml, Germany) were applied through a stiff micropipettor tip with a 2-mm opening positioned 10–15 mm above the skin in the area of ~ 2 cm^2. The controlled air pressure at the animal's skin surface was 1.139 g/cm^3. A plastic cover with 2-cm holes was placed above the rat's body to restrict the area of stimulation. The micropipettor was attached to a switch which sent a 5 V TTL signal to the recording system every time the air flow started and ended; in this way, a very precise temporal alignment of stimuli onset and recorded neurons activity was achieved.

3.3.2. Oxytocin and PVN neurons responses to 'airpuffs'

Airpuffs were delivered repeatedly on the rat's skin on three areas of back (anterior, central, posterior), on two areas of the ventral side (abdomen, ano-genital region), and on whiskers. Stimulation of the in three areas of the back with airpuffs produced a prompt and reproducible increase of oxytocin neurons activity in 19 cells over the 23 recorded (87%). The average increase of firing rate after stimuli onset was 1.3 $\pm$ 0.5 spikes/s ($p = 0.02$, $n = 19$) with respect to baseline; the delay of the response varied among cells: 10 out of 19 cells responded with a short delay (average delay 500 $\pm$ 100 ms), while the remaining 9 cells responded with delay in the order of seconds. By contrast, airpuffs applied onto the abdomen produced only a very moderate change of oxytocin cell firing (average firing rate change 0.4 $\pm$ 0.3 spikes/s, $n = 14$, not significant), and no oxytocin neuron responded significantly to airpuffs applied to the whiskers ($n = 10$) or to the anogenital area ($n = 12$).

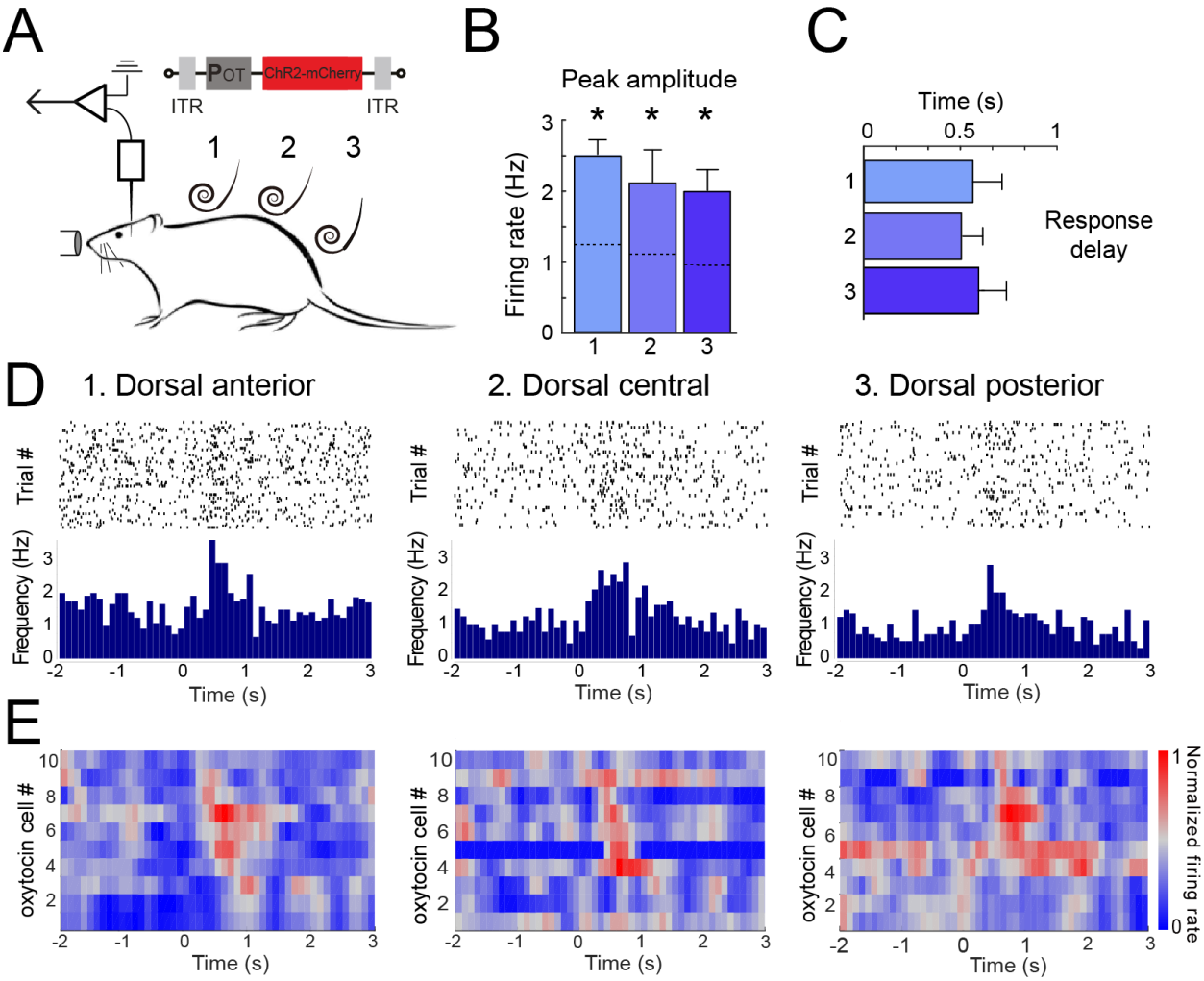

Figure 3.5 Oxytocin neurons response to somatosensory stimulations

*(**A**) Head-fixed and lightly anesthetized rats injected with rAAV-OTp-ChR2-mCherry were stimulated with airpuffs on the anterior (1), central (2), and posterior (3) parts of back, while oxytocin cells activity was recorded with an optoprobe. (**B**) Peak (maximum) amplitude of oxytocin neurons spiking activity after airpuff stimulations; dashed line is average firing rate 2 seconds before stimulus onset. (**C**) Average response delay of oxytocin neurons to airpuff stimulations. (**D**) PSTHs example of oxytocin cell responses to airpuffs applied to the rat's back. (**E**) Heatmaps of normalized PSTHs of 10 (out of 23) recorded oxytocin cells response to airpuffs in three regions of the back.*

I recorded also the activity of PVN non-oxytocin neurons and some of them showed some modulation of firing rate upon stimulation; 17% of the cells showed an increase in firing rate similar to the one registered by oxytocin neurons, 9% showed a decrease in spiking activity, and the remaining 74% did not manifest any significant change.

3.3.3. Oxytocin neurons do not respond specifically to pheromone olfactory cues

To evaluate if oxytocin neurons respond to olfactory and, in particular, pheromone cues, I recorded the spiking activity before, during, and after exposing the animal to the smell of beddings with urine from a female conspecific, or clean beddings as control. Neuronal activity is than aligned to onset of the stimuli and analyzed. None of the recorded oxytocin neurons showed a significant change in spiking activity or spike pattern after smell exposure to urinated nor clean beddings. The average change of firing rate was not statistically different from zero (average difference from baseline: 0.3 ± 0.7 spikes/s, $p = 0.34$ n.s.); the same was true for the index of dispersion (average difference from baseline: 0.2 ± 0.3, $p = 0.48$ n.s.).

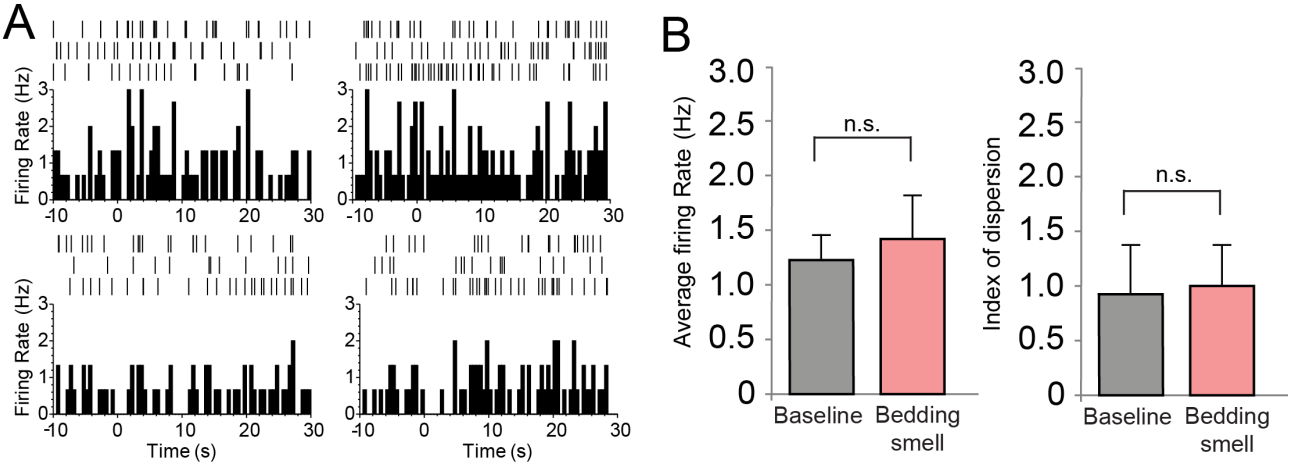

Figure 3.6 Olfactory response of oxytocin neurons to urinate beddings smell.

*(**A**) PSTHs of oxytocin neurons spiking activity aligned to onset of olfactory cues; no significant changes in firing rate are detected. (**B**) Average firing rate and index of dispersion of oxytocin neurons 10 s before presentation of the olfactory stimuli vs 10 s after. All data show average + SEM.*

3.4. Functional oxytocinergic microcircuit within the PVN

Recording of PVN oxytocin neurons during social interactions and during 'airpuff' stimulations suggested that somatosensory stimuli are necessary and sufficient to trigger an increase in spiking activity in most of the recorded neurons. In the light of these results, is natural to ask whether somatosensory inputs from the periphery equally reaches all PVN oxytocin neurons or if this information is mainly conveyed to a subpopulation of oxytocin neurons. To answer this question, I started by looking at the expression of the IEG

(immediate early gene) c-Fos, a marker of neuronal activity, in PVN oxytocin neuron after repetitive tactile stimulations.

3.4.1. c-Fos expression in oxytocin neurons

The expression of the c-Fos in oxytocin neurons has been extensively studied (Brown *et al.*, 2013): the expression of this gene in OT neurons is correlated with the average firing rate of the cell, but is not necessarily correlate to the peptide secretion rate. Indeed, oxytocin cells show a robust expression of c-Fos when there is a sustained increase of firing activity over time, which can occur, for example, in response to increase of osmotic stimulation (salt loading), administration of CCK (cholecystokinin), or fear exposure. By contrast, during other physiological events such as lactation, there is a re-organization of spike activity into bursts without increase of in the average activity level (Rossoni *et al.*, 2008). Thanks to the non-linear relationship between inter-spike intervals and oxytocin secretion rate, the re-organization of the firing activity causes pulsatile axonal release of high amounts of oxytocin into the posterior pituitary gland, necessary for milk ejection, but do not induce any detectable increase in the expression of c-Fos in the cells. This observation is critical to understand to the following results on c-Fos expression in a specific subpopulation of oxytocin neurons induced by somatosensory stimulations.

3.4.2. Airpuffs induced c-Fos expression in parvocellular OT neurons

To understand which subpopulation of oxytocin neurons is primarily activated by sensory stimuli, I first looked at the expression of the immediate early gene c-Fos in oxytocin neurons after repetitive “airpuff” stimulations to the back of awake and non-anesthetized rats. Eight rats were injected with the marker of magnocellular neurons Fluorogold and they were trained for one week for short-term immobilization to avoid any interference with stress. After the animals got use to the immobilization procedure, four of them were stimulated for 10 minutes with repetitive and controlled puffs of pressurized air on the fur on various spots on the back of the animal. The other four rats were not stimulated and served as controls. 90 minutes after the stimulation, the animals were killed by overdose of isoflurane and transcardially perfused. The brains were extracted, sliced, and stained with antibodies against Fluorogold, c-Fos, and oxytocin. The histological analysis revealed the presence of c-Fos immunosignal in (30 $\pm$ 4) % of parvocellular (99 out of 337 cells in 4 rats) but not in magnocellular oxytocin neurons (0.9 $\pm$ 0.6 % 18 out of 2080 cells in 4 rats), in the stimulated

rats. Virtually no c-Fos (0.7 ± 0.2 %, 14 out 1959 cells in 4 rats) signal was detected in any oxytocin neurons in the non-stimulated control rats.

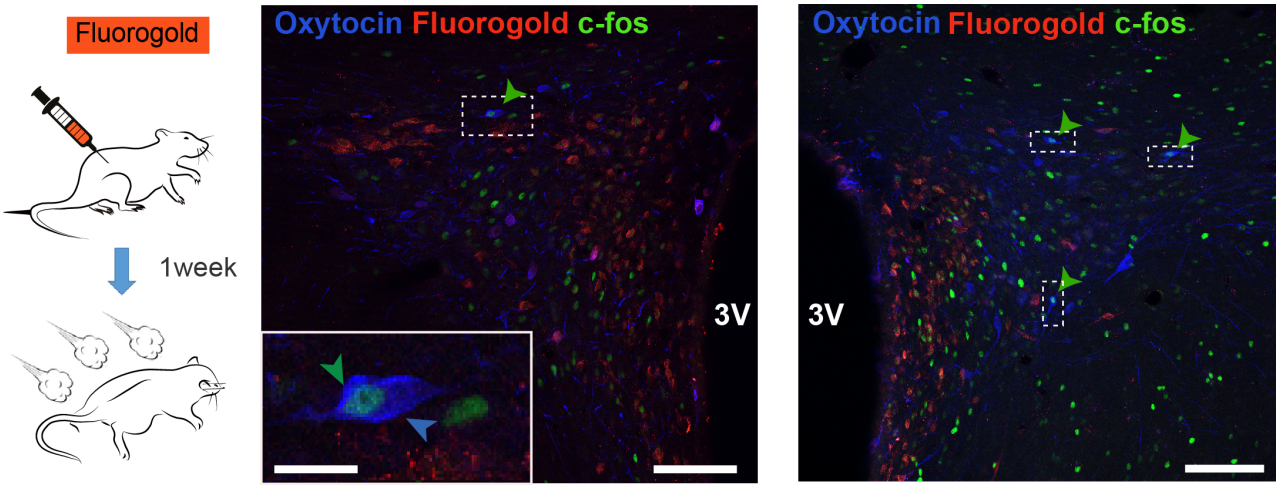

Figure 3.7 c-Fos expression in parvocellular OT neurons following somatosensory stimulation

Fluorogold-injected rats received continuous 'airpuff' stimulations for 10 min, then were sacrificed and perfused 90 min later. PVN coronal slices were triple-stained with antibodies against oxytocin (blue), fluorogold (red) and c-Fos (green). The image on the left shows a (fluorogold-negative) parvocellular oxytocin cell expressing c-Fos (one of 99 such double-labeled cells observed in 4 rats) with respective enlargement of the cell. The image on the right shows 3 parvocellular oxytocin cells expressing c-Fos. Scale bars = 100 µm and 10 µm (inset).

The fact that c-Fos signal in stimulated rats was detected only in parvocellular and not in magnocellular OT neurons suggests that the first population is strongly activated by the stimuli (only a sustained increased of spiking activity can induce c-Fos expression in OT neurons, as mentioned in the previous paragraph), while the latter population display a re-organization of the spiking pattern, that is sufficient to trigger oxytocin release but not to induce a significant increase in c-Fos expression.

Therefore, our hypothesis is that the population of parvocellular oxytocin neurons is firstly and strongly activated upon somatosensory stimuli and that these neurons subsequently recruit and modulate the activity of magnocellular oxytocin neurons.

3.4.3. Parvocellular oxytocin neurons activate PVN magnocellular oxytocin neurons

I illustrated the evidences that parvocellular oxytocin neurons are primarily activate upon somatosensory stimulation and that recorded PVN OT neurons (likely magnocellular neurons) show increased spiking activity after 'airpuffs' application, which suggest the existence of a functional intra-PVN oxytocin neural network. To further investigate the relationship between PVN OT neurons, I aimed to record the oxytocin neurons population while manipulating the activity of parvocellular oxytocin neurons with the DREADD system. Following the observation from previous studies (Eliava *et al.*, 2016) that parvocellular oxytocin neurons in the PVN project to the SON, we labeled them retrogradely by injecting the canine adenovirus CAV2-Cre into the SON concomitantly with Cre-responder AAV expressing the DREADD proteins (hM3Dq or hM4Di) under the control of the oxytocin promoter into the PVN. At the same time, we injected the AAV OTp-GCaMP6s in order to express the calcium indicator GCaMP6s virtually in all PVN oxytocin neurons.

With this combination of viral vectors, we could selectively activate (hM3Dq) or silence (hM4Di) parvocellular oxytocin neurons by injecting CNO (3 mg/kg, i.p.) while monitoring the general population of oxytocin neurons (mainly magnocellular neurons) via fiber-photometry. Activation of the parvocellular oxytocin cells induced an increase in Ca^{2+} fluorescent signal of oxytocin neuron population after 60 minutes and lasting for more than 30 minutes (33 $\pm$ 8 % increase of the area under the curve (AUC), $p = 0.03$, $n = 3$). Conversely, silencing the parvocellular oxytocin neurons decreased Ca^{2+} fluorescent signal of the general population after circa 30 min and lasting for more than 60 minutes (67 $\pm$ 11 % decrease of AUC, $p = 0.007$, $n = 3$). Average calcium traces of recorded oxytocin neurons following activation or silencing of parvocellular oxytocin neurons are depicted in Fig 3.8. Considering that the contribution of parvocellular oxytocin neurons to the oxytocin population calcium signal is negligible, those results suggest that changes in parvocellular neurons activity directly influence the firing pattern of at least a good portion of PVN magnocellular oxytocin cells.

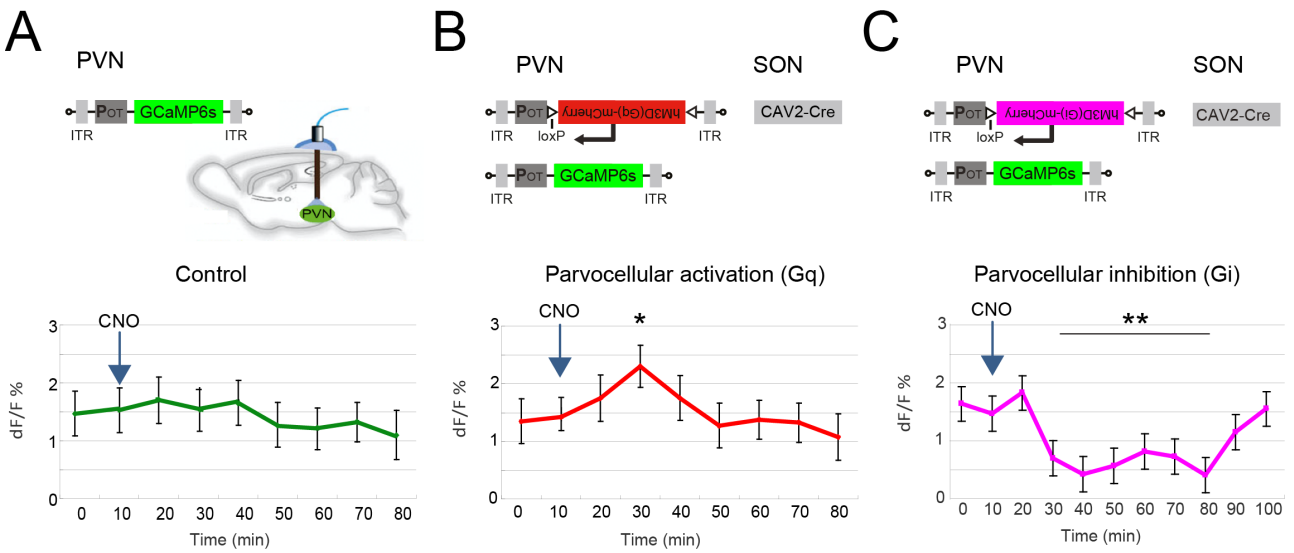

Figure 3.8 Chemogenetic activation of parvocellular oxytocin neurons

*Top: schema of viral vectors injected for fiber photometry recording of PVN oxytocin neurons calcium activity in basal conditions (**A**), or with concomitant CNO-induced activation (**B**) or silencing (**C**) of parvocellular oxytocin neurons expressing designer receptors (Gq and Gi, respectively). Bottom: time series of fiber photometry Ca^{2+} recording of oxytocin neurons before and after i.p. injection of CNO. All data points are cumulative values for each 600-s time bin (* $p < 0.05$, ** $p < 0.01$). Activation, $p = 0.03$, inhibition, $p = 0.004$, $N = 3$ per group. All data show average ± SEM.*

The exact mechanism of communication between parvocellular and magnocellular oxytocin neurons is unknown, but is known that oxytocin neurons can interact via somato-dendritic release of oxytocin and via intrahypothalamic glutamatergic synapses (oxytocin neurons highly express VGluT2) (Johnson and Young, 2017). Direct synaptic contacts of parvocellular oxytocin neurons in the PVN and magnocellular oxytocin neurons in the SON have been demonstrated by simultaneous electrophysiological recordings and by electron microscopy imaging (Eliava *et al.*, 2016). In the light of our results, it's reasonable to think that electrical coupling between parvocellular and magnocellular oxytocin neurons within the PVN also exists. Further evidences come from high magnification confocal images of the PVN of those rats whose parvocellular oxytocin neurons have been labeled with a fluorescent marker (mCherry) and the general population of oxytocin neurons with a different marker (GFP). In those images we could see axons of parvocellular oxytocin neurons (expressing both markers) innervating the PVN and forming close appositions to the somata and dendrites of magnocellular oxytocin cells (see figure 3.9). Electrophysiological

recordings of PVN magnocellular oxytocin neurons and simultaneous stimulation of parvocellular neurons in *ex-vivo* brain slices are currently in progress.

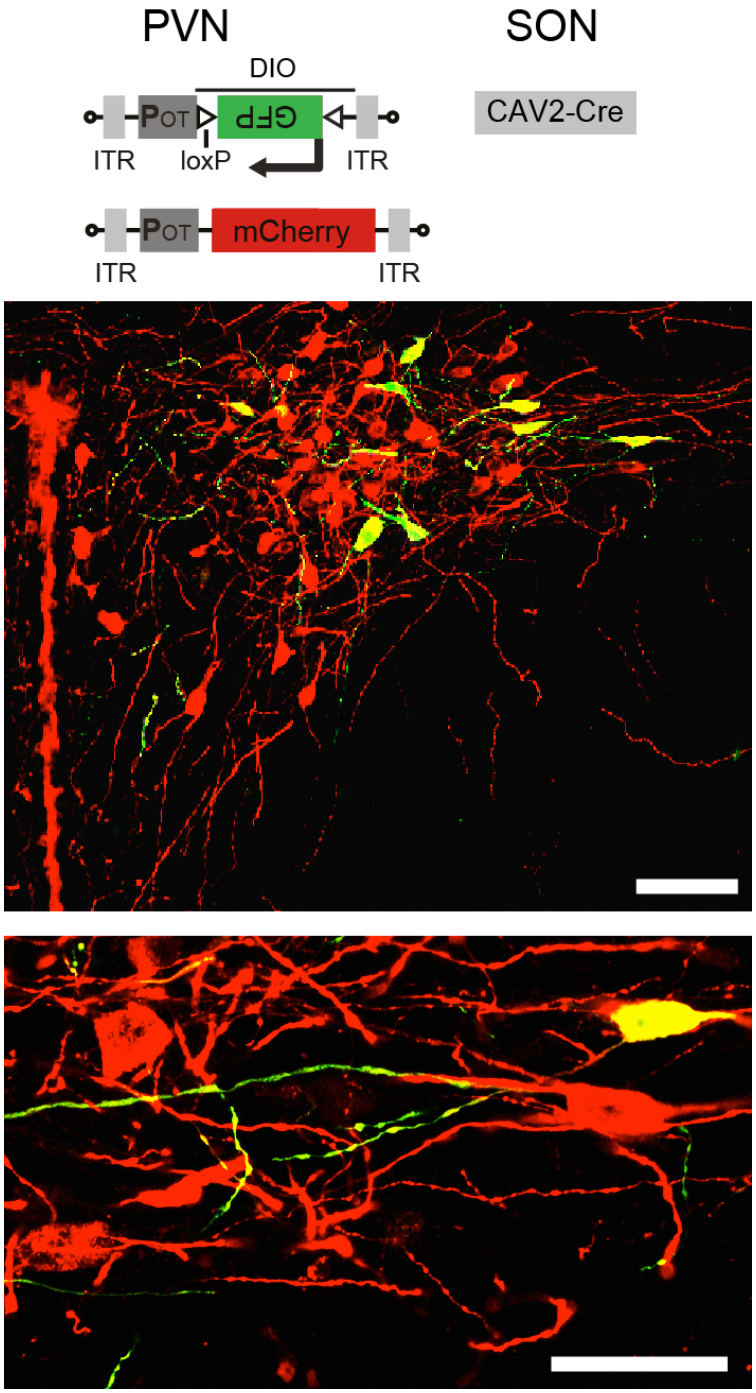

Figure 3.9 Putative PVN connection between parvocellular and magnocellular oxytocin neurons

Schema of injected viral vectors: CAV2-cre was injected bilaterally in the SON; OTp-DIO-GFP and OTp-mCherry were injected bilaterally in the PVN. Putative parvocellular oxytocin neurons in the PVN (identified by their retrograde labelling from the SON) will express both markers GFP and mCherry and will appear in yellow color, while magnocellular oxytocin

neurons were labeled in red. Confocal images of showing synaptic-like connections between fibers from parvocellular oxytocin neurons (green) and processes (dendrites) of magnocellular oxytocin neurons (red). Scale bars: 100 µm (top panel) and 30 µm (bottom panel).

3.4.4. Manipulation of parvocellular oxytocin neurons influences magnocellular oxytocin neurons response to 'airpuff' stimulations

Given that chemogenetic manipulation of parvocellular oxytocin neurons influences the activity of magnocellular oxytocin neurons within the PVN, we wanted to investigate whether the alteration of parvocellular oxytocin neurons excitability have an effect on airpuffs-evoked responses. With the same viral strategy adopted in the previous experiment, we selectively activate (hM3Dq) or silence (hM4Di) parvocellular oxytocin neurons while simultaneously stimulating the skin on the back of the rat with 'airpuffs' and recording the calcium-depended activity of the general oxytocin neuron population via fiber-photometry.

Stimulus evoked calcium signal responses in control condition (saline injection) versus CNO-induced activation or silencing of parvocellular oxytocin neurons were compared. As depicted in FIG, the activation of parvocellular oxytocin neurons induced an increase in calcium responses resulting in an average increase (peak response, compared to control) of 1.2 $\pm$ 0.2 % of dF/F fluorescent signal after onset of the stimuli and an average increase of 45 $\pm$ 9 % of the relative area under the curve (AUC). Oppositely, silencing of parvocellular oxytocin neurons suppressed stimuli evoked calcium responses resulting in an average decrease of 0.8 $\pm$ 0.1 % of dF/F fluorescent signal and an average decrease of 70 $\pm$ 5 % of the relative AUC after onset of the stimuli with respect to control condition. These results suggest that parvocellular oxytocin neurons play a crucial role in modulating magnocellular oxytocin neurons response to somatosensory stimuli and that a pharmacological alteration of their excitability influences the activity of PVN oxytocin neurons.

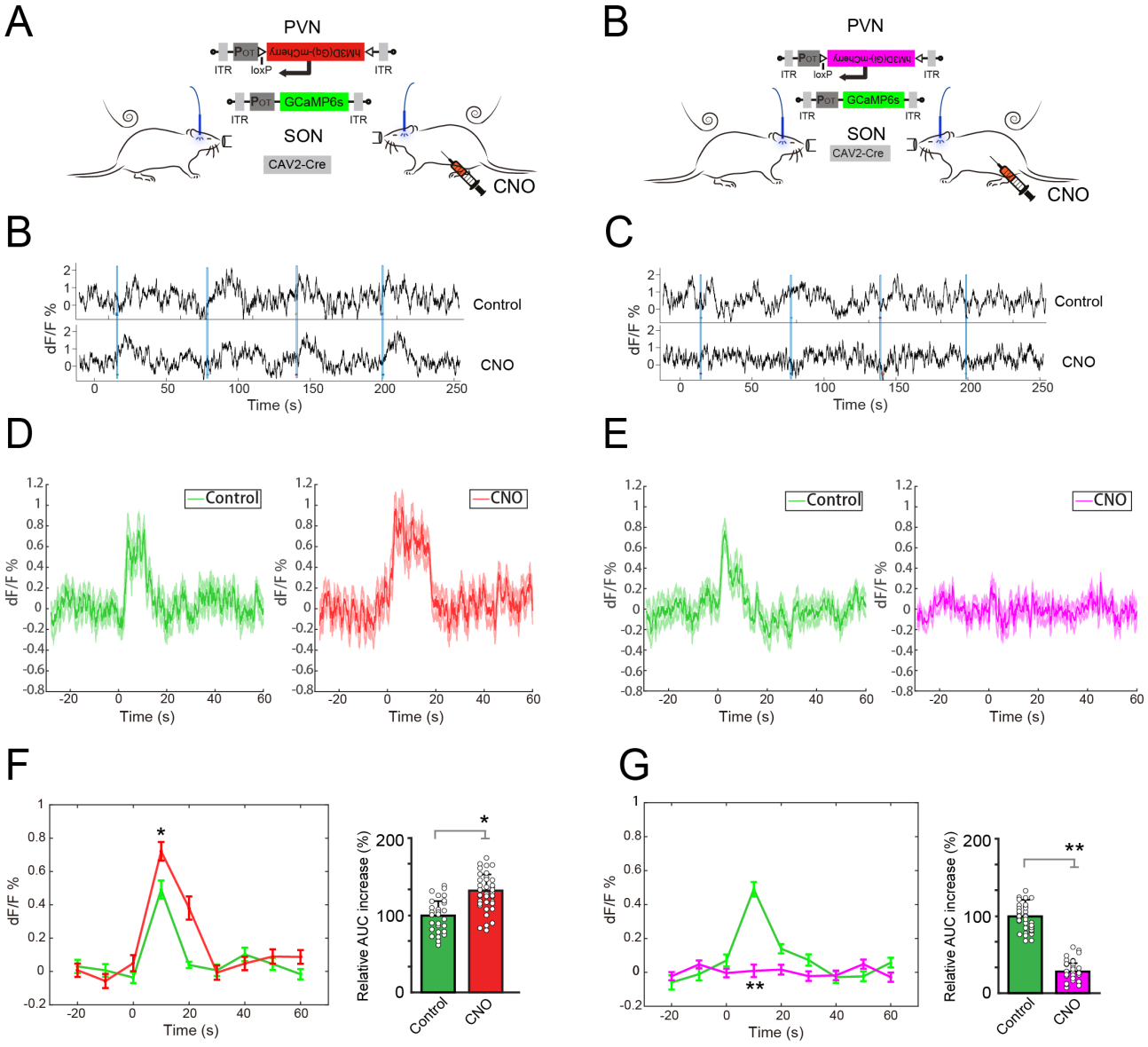

Figure 3.10 Oxytocin neurons response to somatosensory stimulations is modulated by parvocellular neurons.

*(**A-B**) Viral vectors schema for recording calcium-dependent signals in GCaMP6s-expressing oxytocin cells during chemogenetic activation (**A**) or silencing (**B**) of parvocellular oxytocin cells.*

*(**B-C**) Examples of fiber photometry-based Ca^{2+} signals of PVN oxytocin neuron population during 'airpuff' stimulations (blue bars). Top: response to airpuffs 30-60 min after saline injection (Control); bottom: response to airpuffs 30-60 min after CNO induced activation (**B**) or silencing (**C**) of parvocellular oxytocin cells.*

*(**D**) Average traces of Ca^{2+} responses to airpuffs 30-60 min after injection of CNO to activate (Gq) parvocellular oxytocin cells, or saline (Control). Each graphic is the average of 33 airpuffs responses (11 airpuffs per animal in N = 3 animals).*

*(**E**) Average traces of Ca^{2+} responses to airpuffs 30-60 min after injection of CNO to silence (Gi) parvocellular oxytocin cells, or of saline (Control). Each graphic is the average of 33 airpuffs responses (11 airpuffs per animal in N = 3 animals).*
*(**F**) Left: 10-s bin average curves of (**D**) panels; right: area under the curve (AUC) 0-30 s after airpuffs, relative to control (* p = 0.03).*
*(**G**) Left: 10-s bin average curves of (**E**) panels; right: area under the curve (AUC) 0-30 s after airpuffs, relative to control (** p = 0.007).*
All data show means ± SEM.

3.5. Manipulation of parvocellular oxytocin neurons alters social behavior

In the previous sections we showed that oxytocin neurons are considerably activated by physical contacts during social interactions and that somatosensory stimulations primarily activate parvocellular oxytocin neurons which transmit the information to and activate the larger population of PVN magnocellular oxytocin neurons. The following step in understanding of the role parvocellular oxytocin neurons within the oxytocin system is investigating the effect of chemogenetic manipulation of those neurons in freely moving and socially interacting rats.

For this purpose, I used, once again, the viral combination of the canine adenovirus CAV2-Cre in the SON and Cre-dependent adeno-associated virus expressing DREADD genes (hM3Dq or hM4Di) selectively in parvocellular oxytocin neurons in the PVN. Three weeks after viral injection, rats were injected i.p. with either CNO or saline solution 60 min before exposure to behavioral tests. First, the experimental rat was introduced alone in the open field arena and let freely explore the environment for habituation and monitoring of locomotor activity. Second, the stimulus rat was introduced in one of the two chambered compartments while the experimental rat was free to approach the conspecific or explore the rest of the arena. Finally, the wall of the chamber containing the stimulus rat was opened to allow free social interaction between the two animals. Video and ultrasounds were recorded during the whole session.

The general results of the experiments indicate that selective manipulation of parvocellular oxytocin neurons affects the time that the experimental rat spent closely interacting with the stimulus rat during free social interactions. By contrast, in the chambered social interaction test, where no physical contact is allowed, the time spent by the experimental rat approaching the chamber with the conspecific was unchanged. Similarly, general

locomotion of the animal in the open field arena did not differ from CNO or saline injected conditions. More specifically, inhibiting the parvocellular oxytocin cells resulted in an average 12 ± 3% reduction of time spent by the experimental animal with the conspecific (37 ± 6 s, over 5-min sessions, $p < 0.001$) during the free social interaction test, while no significant difference (2 ± 5 s, $p = 0.13$ n.s.) in approaching time was detected during the chambered social interaction test. Conversely, CNO-induced activation of parvocellular oxytocin neurons led to more social interaction: in the free social interaction test, the time spent with a conspecific increased by 5 ± 2% (15 ± 6 s, over 5-min sessions, $p = 0.04$). In the chambered social interaction test, again no significant differences in approaching time was measured between CNO- and saline-injected rats (2 ± 6 s, $p = 0.19$ n.s).

Detailed analysis of free social interactions revealed that chemogenetic inhibition or activation of the parvocellular oxytocin cells had the strongest impact on mounting behavior with opposite effects in the respective cases. Moreover, after silencing the parvocellular oxytocin neurons, experimental rats often actively avoided contacts with the stimulus rat, a behavior hardly ever observed in the saline-injected group.

As an additional control for these experiments, we injected a group of rats with the control virus OTp-DIO-GFP expressing the fluorescent marker GFP in parvocellular oxytocin cells instead of the DREADD protein. No behavioral or locomotive differences were detected in this group of animals when they were injected with CNO versus saline.

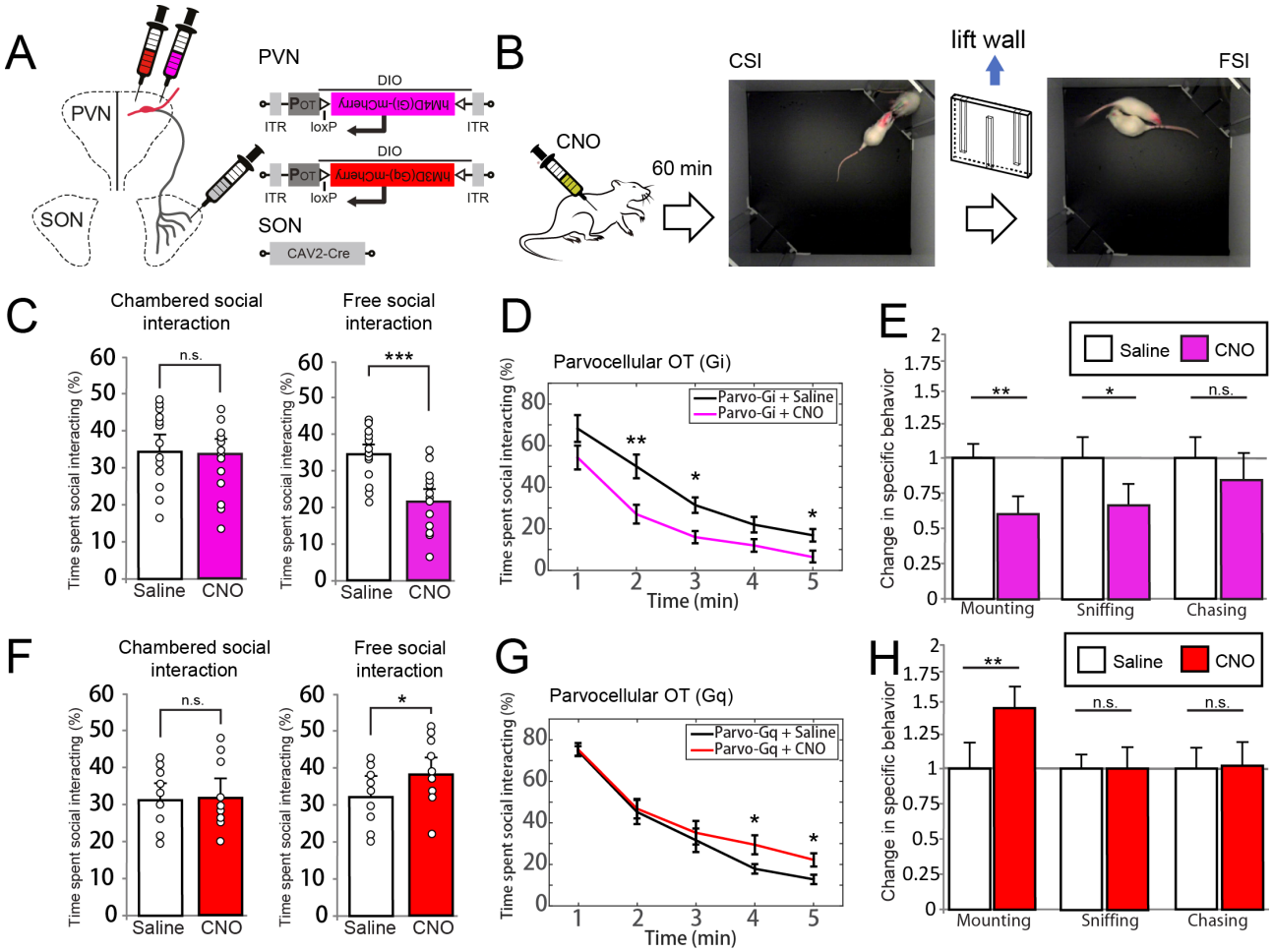

Figure 3.11 Pharmacogenetic manipulation of parvocellular oxytocin cells alters social behavior.

*(**A**) Viral vectors (OTp-DIO-hM3D(Gi)-mCherry or OTp-DIO-hM4D(Gq)-mCherry) used to express gene of interests in parvocellular oxytocin cells.*

*(**B**) CNO or saline was injected i.p. 60 min before the CSI and FSI tests.*

*(**C**) Silencing of parvocellular oxytocin cells (Parvo-Gi group): percentage of time spent by an experimental rat injected with saline or CNO socially interacting with a conspecific in CSI (N = 15, p = 0.004) and FSI (N = 15, p < 0.001, paired t-test), calculated over the 5-min session.*

*(**D**) Temporal dynamics of time spent in social interaction in 1-min bins (2nd minute, p = 0.01, 3rd minute p = 0.03, 5th minute p = 0.04, two-way ANOVA time x treatment).*

*(**E**) Parvo-Gi group: time spent in different social behaviors in rats injected with either saline or CNO: mounting (** p = 0.008), sniffing (* p = 0.012), chasing (p = 0.13 n.s.), N=15, one-way ANOVA Tukey's corrected post-hoc comparison.*

*(**F**) Activation of parvocellular oxytocin cells (Parvo-Gq group): average time spent in social interaction with conspecific stimulus in CSI (N = 9, p = 0.05) and FSI (N = 9, p = 0.04, paired t-test) after CNO or saline injection.*

*(**G**) Temporal dynamics of time spent in social interaction in 1-min bins for rats injected with CNO or saline (4th minute, p = 0.03, two-way ANOVA time x treatment).*
*(**H**) Parvo-Gq group: time spent in different social behaviors in rats injected with saline or CNO: mounting (** p = 0.006), sniffing (p = 0.44 n.s.), chasing (p = 0.27 n.s.), N=9, one-way ANOVA Tukey's corrected post-hoc comparison. All data show means ± SEM.*

3.5.1. Pharmacological OTR blockade decreases social interaction

To prove that alterations of social behaviors induced by DREADD based manipulation of parvocellular oxytocin neurons is indeed an effect mediated by oxytocin release, the same experiment was repeated while applying an oxytocin receptor antagonist, des-Gly-NH_2,d$(CH_2)_5$[Tyr(Me)^2,Thr^4]OVT (Manning *et al.*, 2001), by intracerebroventricular (i.c.v.) microinjection; the dosage used was 0.75 μg/ 5 μl (Neumann *et al.*, 2013; Grund *et al.*, 2017).

Two groups of animals were injected with the viral combination of the canine adenovirus CAV2-Cre in the SON and Cre-dependent adeno-associated virus expressing the excitatory DREADD genes hM3Dq (experimental group) or GFP (control group) exclusively in parvocellular oxytocin neurons in the PVN. The two groups of animals were also implanted with cannulas for i.c.v. injections. Before behavioral tests, the rats received both a i.p. injection of CNO or saline solution (60 min prior to social interaction) and a i.c.v. infusion of oxytocin receptor antagonist or saline (30 min prior to social interaction). All the possible combinations were tested and are summarized in the following table:

	Intraperitoneal	**Intracerebroventricular**
Subgroup 1	Saline	Saline
Subgroup 2	CNO	Saline
Subgroup 3	Saline	OTR antagonist
Subgroup 4	CNO	OTR antagonist

Exactly as in the previous behavioral experiments, rats were placed in an open field arena with a novel stimulus conspecific and social interaction time was measured by analyzing the recorded videos.

In the first group of rats, that is expressing the DREADD excitatory Gq receptor in parvocellular oxytocin neurons, i.c.v. administration of oxytocin receptor antagonist had a pronounced effect on social behavior which was considerably reduced (subgroup 3, 54 ± 17

s, p = 0.007) with respect to matched saline control (subgroup 1, 90 ± 19 s). The decrease of social interaction time was very similar also in presence of the DREADD agonist CNO (subgroup 4, 56 ± 16 s, p = 0.009); on the other hand, injection of CNO alone (subgroup 2, 105 ± 15 s, p = 0.04) is able to increase the time spent by the experimental rat social interacting with the stimulus rat by activating the DREADD-Gq receptor in parvocellular oxytocin neurons. This result confirms that the downstream effect on CNO-induced activation of parvocellular neurons on social behavior is indeed mediated by oxytocin and its receptors.

In the second group of rats, expressing GFP in parvocellular oxytocin neurons, administration of oxytocin receptor antagonist also had a comparable effect in reducing social behavior; however, as expected, CNO itself did not have any effect on social interaction in this group, because the DREADD gene was not present.

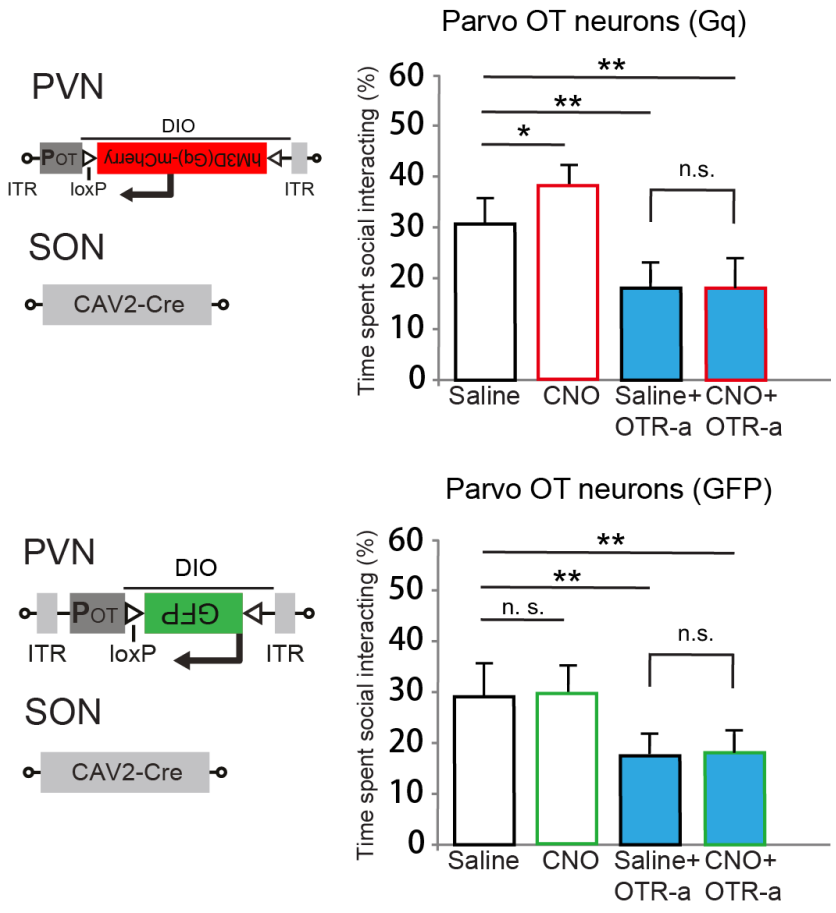

Figure 3.12 OTR-antagonist local infusion decreases social interaction even in presence of pharmacological activation of parvocellular oxytocin neurons.

Percentage of social interaction time in different conditions: saline (control), CNO, OTR-antagonist, or CNO + OTR-antagonist administration. Time spent social interacting over 5-minute sessions.

*Top panel: parvocellular oxytocin neurons express Gq-DREADD. Subgroup 1: 90 ± 19 s, subgroup 2: 105 ± 15 s, * p = 0.04, subgroup 3: 54 ± 17 s, ** p = 0.007, subgroup 4: 56 ± 16 s, ** p = 0.009, one-way ANOVA Tukey's corrected post-hoc comparison.*

*Bottom panel: parvocellular oxytocin neurons express GFP. Subgroup 1: 88 ± 18 s, subgroup 2: 89 ± 14 s, n.s., subgroup 3: 53 ± 14 s, ** p = 0.008, subgroup 4: 57 ± 15 s, ** p = 0.001, one-way ANOVA Tukey's corrected post-hoc comparison. All data show means ± SEM.*

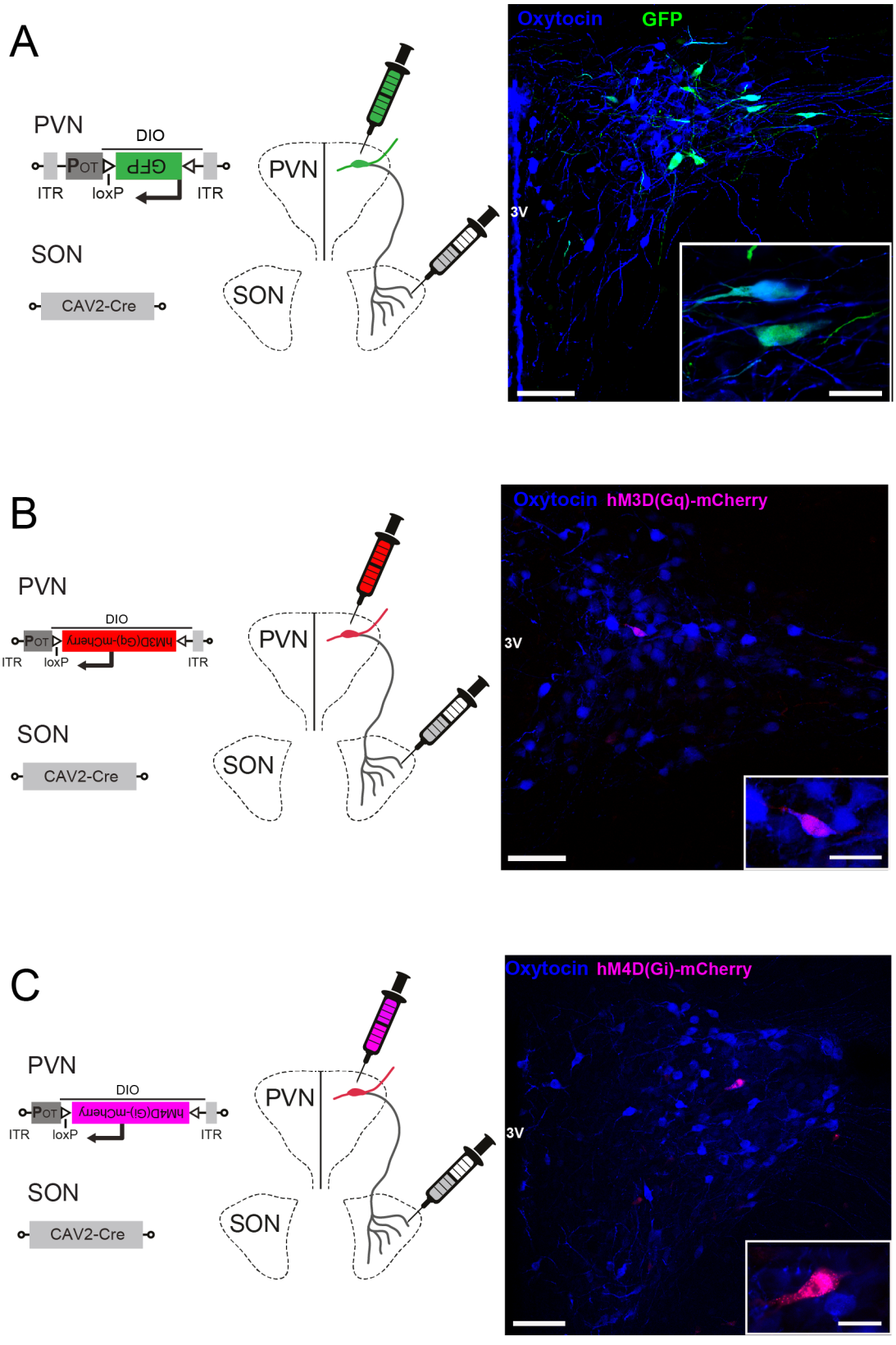

Figure 3.13 Retrograde labeling of parvocellular oxytocin neurons from the SON

*(**A**) Schema of injected viral vectors used to selectively express gene of interests (GFP, hM3D(Gq)-mCherry, or hM4D(Gi)-mCherry) in parvocellular oxytocin neurons. Immunostained PVN sections images showing co-labeling of GFP (green) in parvocellular oxytocin neurons together with OT antibody (blue). (**B**) Immunostained section of PVN*

*showing co-labeling of Gq-mCherry (red) in parvocellular oxytocin neurons together with OT antibody (blue). (**C**) Immunostained PVN section showing co-labeling of Gi-mCherry (red) in parvocellular oxytocin neurons together with oxytocin antibody (blue). Scale bars: 100 µm (main panel) and 30 µm (insets).*

Chapter 4: Discussion

4. Discussion

4.1. Oxytocin and Social interaction

Oxytocin plays a crucial role in a large variety of behaviors essentials for survival and reproduction, many of which involve social interaction between conspecifics. The action of oxytocin in the brain has been proved to regulate a multitude of social behaviors, including social memory (Sanchez-Andrade and Kendrick, 2008), social recognition (Engelmann *et al.*, 1998), play behaviors (Lee *et al.*, 2010), bonding and parental behaviors (Caldwell *et al.*, 2008), sexual behaviors (M.Witt, 1995), and aggression (Bosch *et al.*, 2004), as well to modulate sensory perception (Grinevich and Stoop, 2018) and socially related sensory cues (Marlin *et al.*, 2015; Oettl *et al.*, 2016). The direct involvement of the oxytocin system in the regulation of social behaviors has been reported in several species, including humans and rodents. Direct measurements of extracellular oxytocin concentration in brain regions relevant for social behaviors, such as the CeA (Dumais, Alonso, Bredewold, *et al.*, 2016) or BNST (Dumais, Alonso, Immormino, *et al.*, 2016), suggest that oxytocin is released in those regions during social investigation of a conspecific. Furthermore, pharmacological manipulation of the oxytocin signal pathway in those brain regions, such as administration of oxytocin receptor antagonist, can decrease social interest and social investigation.

Despite the large amount of data available on oxytocin and social behaviors, up to now, no direct electrophysiological recording of oxytocin neurons in socially behaving animals was yet performed. In this work, I presented the first direct recording of single oxytocin neurons in freely moving and socially behaving female rats. Identification of oxytocin neurons among the population of extracellularly recorded PVN neurons was possible thanks to the combination of viral vectors, optogenetic, and spike sorting algorithm. Adeno-associated viruses have been injected into the PVN to transduce the expression of the light-sensitive ion channel Channelrhodopsin2 in oxytocin neurons exclusively. Silicon probe electrodes combined with an optic fiber allowed to simultaneously record extracellular action potential and activating oxytocin neurons via blue light pulses, enabling for identification of those neurons among other PVN cells. Finally, spike sorting algorithm permitted to discriminate individual neurons recorded during freely moving behaviors.

The results of these experiments suggest that non-aggressive social behavior in female rats and, in particular through physical contacts, elicit a coordinated, clustered spiking activity of PVN oxytocin neurons. This activity is nearly-synchronous across recorded OT neurons and

it is highly correlated with theta rhythmicity of PVN local field potential. Those coordinated changes in electrical activity of oxytocin neurons occurred only during free social interaction, in which physical contacts between conspecifics was allowed, but not during chambered social test when the interaction between animals was limited by a barrier that prevent physical touch. In addition, the total amount of oxytocin released by the recorded neurons was estimated based on their spiking activity by using a mathematical model developed on comprehensive studies on activity-dependent peptide secretion from magnocellular neurosecretory cells, and revealed that the highest released rate occurred during social interaction when several physical contacts occurred.

4.2. Oxytocin and the sensory system

Social behaviors are complex interactions between individuals that involve processing of sensory information coming from different perception systems in a dynamic and context specific manner (Veenema and Neumann, 2008).

In the present work, I aimed to dissect the different sensory component that contribute to activate oxytocin neurons during social interaction. Experimentally, this was achieved by presenting in a repeated and controlled manner specific stimuli, either tactile, olfactive, or auditive while recording oxytocin cells spiking activity in lightly anesthetized rats. Of all stimulation classes, only the somatosensory one was able to induce a pronounced and reproducible increase in oxytocin neurons spiking activity. Repeated compressed air-delivered stimulations (‘airpuffs’) applied on the skin on different parts of the rat body induced different responses in oxytocin neurons activity: the highest response, up to 3-fold increase, was triggered when stimulating the skin on the caudal portion of the back. The same type of stimulation applied to awake immobilized rats, induced an increase of immediate early gene *Fos* in a specific subpopulation of oxytocin neurons, named parvocellular oxytocin neurons.

Other type of sensory stimulations, such as exposure to urine and beddings smell (olfactory), to playback of recorded ultrasound vocalizations (auditory), or to the sight of a conspecific through a transparent barrier (visual) did not elicit any significant change in oxytocin neuron spiking activity. Therefore, is to conclude that oxytocin neurons are preferentially activated by tactile stimulations.

4.3. The role of parvocellular oxytocin neurons

The population of parvocellular oxytocin neurons is known to have different connectivity, cellular morphology, and projection site with respect to the more abundant population of magnocellular oxytocin neurons (Althammer and Grinevich, 2018), and it is involved in inflammatory pain processing and nociception via action on WDR (wide dynamic range) neurons in the deep layers of the spinal cord (Eliava *et al.*, 2016). In addition to that, it was shown that parvocellular oxytocin neurons (which reside exclusively in the PVN) project onto magnocellular oxytocin neurons of the SON.

As discussed in the previous paragraph, the general population of oxytocin neurons (that is formed, in large proportion, by magnocellular neurons) is responding to repetitive somatosensory stimulations, but only parvocellular oxytocin neurons display an increase in *c-Fos* (marker of neuronal activity) expression following the same type of stimulations. These two pieces of information combined opened a question on the role of parvocellular neurons in the responsiveness of the oxytocin system to tactile stimuli. To investigate on that, I recorded the overall activity of PVN oxytocin neurons by transfecting them with the genetically encoded calcium indicator GCaMP6s and by measuring the calcium activity-dependent fluorescent changes of oxytocin neurons via fiber photometry in response to 'airpuffs' stimulations. After that, I selectively excited or inhibited the activity of parvocellular oxytocin neurons with DREADD pharmacology: the stimulus-dependent response of PVN oxytocin neurons was enhanced when parvocellular neurons were activated and it was drastically reduced when parvocellular neurons were inhibited.

Finally, I examined the effect of pharmacological manipulation of parvocellular oxytocin neurons (again with DREADD based system) on social behavior. Gi-mediated inhibition of parvocellular oxytocin neurons resulted in a pronounced decrease of time spent by the experimental rat socially interacting with the conspecific stimulus. On the other hand, Gq-mediated activation of parvocellular oxytocin neurons resulted in an increase of social interaction time. The changes in time spent by the rats in social contact occurred exclusively during the free social interaction paradigm, in which the animals were allowed to have physical contacts with each other, but not did not influenced the social investigation time in the chambered social interaction test, where animals were separated by a barrier.

To evaluate whether these effects were actually mediated by oxytocin signaling, the experiment was repeated in conjunction with local infusion of oxytocin receptor antagonist in the brain via a chronically implanted cannula. The pharmacological blockade of OT receptors produced a decrease of social interaction time that was not rescued by

simultaneous activation of parvocellular oxytocin neurons. In conclusion, parvocellular oxytocin neurons appear to be directly involved in the processing of somatosensory information and they are able to orchestrate magnocellular oxytocin neurons activity and consequently modulate oxytocin release in other brain regions that are involved in social behavior.

4.4. Applications of oxytocin research in clinical psychiatry

In this work, I presented novel insights on the role of oxytocin and somatosensory stimulations in regulating social behavior in an animal model. These findings may have implications for understanding and treating mental disorders characterized by social and/or affiliative deficits.

In healthy individuals, oxytocin is crucially involved in various aspects of human behavior such as social cognition, affectivity, stress response, affiliation, and prosocial behavior. Intranasal oxytocin administrations in double blind placebo controlled trials has been shown to increase social interaction, empathy and trust, and to reduce stress levels in healthy subjects (Veening and Olivier, 2013). Due to these properties oxytocin is considered a promising pharmacological candidate to improve sociality, socio-communication and, ultimately, patients' well-being in a number of mental disorders including autism spectrum disorders (ASD) (Guastella *et al.*, 2010; Okamoto *et al.*, 2016), schizophrenia (Averbeck *et al.*, 2012), emotional disorders (Rutter *et al.*, 2019), antisocial personality disorders (ASPD) (Gedeon, Parry and Völlm, 2019), depression, and anxiety (Watanabe *et al.*, 2014).

4.4.1. Oxytocin and autism

Social and communications deficits in humans are core symptoms of several neurological disorders including autism spectrum disorders. Autism is a neurodevelopmental condition characterized by social deficits, absent or impaired communication, and tendency to repetitive behavior. The onset of ASD is typically in early childhood (one to three years of age) and generally persist throughout the whole life (Higashida *et al.*, 2019). The prevalence of ASD is high (estimated global prevalence ~1-2 % (Elsabbagh *et al.*, 2012)) and no effective treatments are currently available to eliminate or mitigate its symptoms, with the exception of irritability, that can be alleviated by risperidone or aripiprazole (McCracken J.T., 2003; Anagnostou, 2018).

Within neuropsychiatric disorders, ASD is among the most heritable, yet the genetic basis of autism is very complex and not attributable to a single gene or to a unique set of

mutations; however, one of the most studied autism candidate genes, *reelin*, has been linked to changes in the expression of OTR in the brain (Liu *et al.*, 2010; LoParo and Waldman, 2015).

Clinical trials on intranasal OT administration suggest that oxytocin has benefits in alleviating social deficits in ASD patients compared to placebo controls, even though the effect size is moderate (Cohen's d = 0.57) (Bakermans-Kranenburg and Van IJzendoorn, 2013).

In conclusions, it seems likely that in the near future oxytocin will be used in the treatment of ASD as an accessory help in conjunction with psychotherapy and dedicated emotional support, but it is still far from being a definitive solution for this complex neuropsychiatric condition.

4.4.2. Oxytocin and the social touch

Physical contacts are fundamental throughout life to create social bonds starting from the attachment of infants to their mothers and developing with social play during childhood and adolescence. In healthy subjects, the tactile channel is a very powerful tool for non-verbal communication of emotions and intentions (Hertenstein *et al.*, 2009). A hug, a massage, a gentle touch of social contacts are generally very pleasant and rewarding events and recent studies have provided insight into how social interaction can generate rewarding experiences by inducing oxytocin release from PVN oxytocin axon terminals in the ventral tegmental area (VTA), a key region of the brain's reward circuitry (Hung *et al.*, 2017).

In contrast to that, mental disorders with social impairments, such as ASD, are usually accompanied by an aversion to social touch (Baranek, Foster and Berkson, 1997; Kern *et al.*, 2006). In fact, ASD patients frequently struggle with both receiving and offering interpersonal touch (Baranek, Cascio and Lorenzi, 2016).

In the present work, I illustrate evidence which suggests that tactile inputs generated by physical contacts during social interactions are essential to elicit coordinate PVN oxytocin neurons activity. These findings may have implications for understanding and treating mental disorders characterized by social and/or affiliative deficits in human patients.

In the light of those observations, it is possible to speculate that in people with neurodevelopmental disorders the lack of social physical contacts or other forms of interpersonal sensory exchange may be caused or may lead to lower rate of oxytocin neurons activity and hence reduced oxytocin release in the so-called "social brain regions", such as the amygdala, the orbitofrontal cortex (OFC), the temporoparietal cortex (TPC), and the insula, among others (Weston, 2019). In turn, lower rate of oxytocin in those brain

regions may results in decline in socio-communicational abilities and aversion to social experiences, ending in a negative loop of anti-sociality and decreased brain oxytocin levels. A key step to break this loop, is to understand the mechanisms by which the oxytocin systems is activated in physiological and in pathological conditions, both in animal models and in human subjects.

Finally, given the importance of tactile inputs to activate oxytocin neurons, is tempting to think about the development of novel therapies designed for people with social disorders that allows to re-establish a positive value to social touch, and, in general, social communication, perhaps in conjunction with pharmacological that can elevate endogenous levels of oxytocin (such as intranasal oxytocin administration). It would be highly intriguing to investigate, whenever the patient tolerates some degree of physical contacts, whether gentle tactile stimulations, such as those induced by social touch, massages, or physical therapy are able to rescue physiological level of oxytocin in the brain and possibly contribute to alleviate social deficit symptoms.

4.5. Conclusion and perspectives

In my thesis I illustrated a series of experiments that had the aim of investigating the electrical properties and the dynamics of activity of a specialized class of neuroendocrine cells, *i.e.* the oxytocin neurons in paraventricular nucleus of the hypothalamus, during exploratory and social behaviors in adult female rats. In the first phase of the experiments, it became clear that PVN oxytocin neurons activity changes during social interaction with a conspecific, with respect to exploratory behavior. More precisely, oxytocin neurons spiking activity increases, the firing pattern changes from regular to clustered, and synchronizes across recorded oxytocin neurons.

Then, I dissected the sensory pathway that preferentially activate PVN oxytocin neurons during social interaction by performing chambered social interaction that prevents physical contacts between animal, but allows the exchange of visual, olfactory, and auditory socially-relevant signals. Precluding somatosensory component of social interaction kept the activity of oxytocin neurons close to basal levels. In line with that, repetitive tactile stimulation of the rat's skin with 'airpuffs' were sufficient to trigger time-locked increase of individual oxytocin neurons in lightly anesthetized conditions.

After that, I investigated the activity chances of oxytocin neurons in response to somatosensory stimulations by looking at the expression of the marker for neuronal activity *c-Fos*, and discovered that a specific subpopulation of PVN oxytocin neurons, the

parvocellular oxytocin neurons, are primarily activated upon intense tactile stimuli. Following that, I examined the role of this population of parvocellular neurons in modulating the activity of the more abundant population of magnocellular neurons in response to 'airpuff' stimulations. Finally, I analyzed the effect of selectively activation or inhibition of parvocellular oxytocin neurons on social behavior, finding that activation leads to an increase in social interaction time while inhibition reduces it.

In all behavioral experiments I employed adult virgin female rats and social interaction were always done between unfamiliar conspecifics of same age and sex. It would be interesting to explore the activity of PVN oxytocin neurons also in other behavioral paradigms, such as social interaction between male and female rats, mother and pups, play behaviors in juvenile rats, or reunion of social isolated animals.

Regarding the intra-PVN oxytocin circuit, I brought evidence supporting the hypothesis that parvocellular oxytocin neurons are able to modulate the activity of PVN magnocellular oxytocin neurons. Further proofs of the existence of this neuronal circuit may be provided from direct electrophysiological recordings of PVN magnocellular oxytocin neurons following optogenetic stimulation of parvocellular neurons in *ex-vivo* brain slice preparation; this experiment is currently in preparation by the team of our collaborator Dr. Alexandre Charlet at the university of Strasbourg. Furthermore, ultra-structural imaging with electron microscopy may give precise anatomical evidence for synaptic connections between parvocellular and magnocellular oxytocin neurons within the PVN.

In my thesis I did not examined the complete neural circuit which allow somatosensory information coming from the peripheral nerves to reach and activate PVN oxytocin neurons. It is known that a group of circa 30 parvocellular neurons send direct projections from the PVN to WDR neurons in deep layers of the spinal cord where they release oxytocin to promote analgesia during acute inflammatory pain. However, direct ascending monosynaptic connections from sensory neurons in the spinal cord to the PVN have not been reported so far. It is possible that spinal cord sensory neurons project to some structures of the brainstem, such as nucleus tractus solitarius (NTS), locus ceruleus (LC), raphe nuclei (RN), and periaqueductal gray (PAG), which in turn project to the PVN. In the study (Köves *et al.*, 2012) the authors injected GFP retrograde virus in the nipple of female rats; the virus was designed to pass synapses - after replication in the neuronal cell body - to the next neuron in a retrograde fashion with a speed of 15 mm/hour. Two days after injection GFP signal was found in neurons of the ipsilateral dorsal root ganglion and lateral horn of thoracic segments of the spinal cord. Three days after injection few labeled neurons

appeared in the brainstem and the hypothalamus. After four days, many oxytocin positive labeled neurons appeared in the PVN, mostly in the parvocellular compartment of the nucleus.

A more precise dissection of monosynaptic inputs to PVN oxytocin neurons – with a focus on differential inputs to parvocellular and magnocellular neurons - using retrograde tracing with rabies virus system (Callaway and Luo, 2015) is currently under examination in our laboratory thanks to the help of Dr. Arthur Lefevre.

Lastly, it would be of great relevance to investigate the relationship between social interactions, somatosensory inputs, and the oxytocin system also in other animal models such as the monogamous prairie voles, which form life-long bonding with their sexual partner and both parents display nursing behavior towards the offspring, and non-human primates, such as the marmosets, which exhibit a richer and more complex set of social behaviors compared to rodent models.

5. References

Aitchison, K. J. *et al.* (2000) 'Clozapine pharmacokinetics and pharmacodynamics studied with CYP1A2-null mice', *Journal of Psychopharmacology*. doi: 10.1177/026988110001400403.

Althammer, F. (2017) *Doctoral dissertation title: Fear memory engram in the hypothalamic oxytocin system*. University of Heidelberg.

Althammer, F. and Grinevich, V. (2018) 'Diversity of oxytocin neurones: Beyond magno- and parvocellular cell types?', *Journal of Neuroendocrinology*. doi: 10.1111/jne.12549.

Amadei, E. A. *et al.* (2017) 'Dynamic corticostriatal activity biases social bonding in monogamous female prairie voles', *Nature*. doi: 10.1038/nature22381.

Anagnostou, E. (2018) 'Clinical trials in autism spectrum disorder: Evidence, challenges and future directions', *Current Opinion in Neurology*. doi: 10.1097/WCO.0000000000000542.

Averbeck, B. B. *et al.* (2012) 'Emotion recognition and oxytocin in patients with schizophrenia', *Psychological Medicine*. doi: 10.1017/S0033291711001413.

Bakermans-Kranenburg, M. J. and Van IJzendoorn, M. H. (2013) 'Sniffing around oxytocin: Review and meta-analyses of trials in healthy and clinical groups with implications for pharmacotherapy', *Translational Psychiatry*. doi: 10.1038/tp.2013.34.

Baranek, G. T., Cascio, C. J. and Lorenzi, J. (2016) 'Self-reported pleasantness ratings and examiner-coded defensiveness in response to touch in children with ASD', *Journal of Autism and Developmental Disorders*. doi: 10.1007/s10803-013-1961-1.

Baranek, G. T., Foster, L. G. and Berkson, G. (1997) 'Tactile Defensiveness and Stereotyped Behaviors', *American Journal of Occupational Therapy*. doi: 10.5014/ajot.51.2.91.

Benelli, A. *et al.* (1995) 'Polymodal dose-response curve for oxytocin in the social recognition test', *Neuropeptides*. doi: 10.1016/0143-4179(95)90029-2.

Blevins, J. E. (2004) 'Evidence that paraventricular nucleus oxytocin neurons link hypothalamic leptin action to caudal brain stem nuclei controlling meal size', *AJP: Regulatory, Integrative and Comparative Physiology*. doi: 10.1152/ajpregu.00604.2003.

Boll, S. *et al.* (2017) 'Oxytocin and Pain Perception: From Animal Models to Human Research', *Neuroscience*. doi: 10.1016/j.neuroscience.2017.09.041.

Bosch, O. J. *et al.* (2004) 'Release of oxytocin in the hypothalamic paraventricular nucleus, but not central amygdala or lateral septum in lactating residents and virgin intruders during maternal defence', *Neuroscience*. doi: 10.1016/j.neuroscience.2003.11.028.

Britt, J. P., McDevitt, R. A. and Bonci, A. (2012) 'Use of channelrhodopsin for activation of CNS neurons', *Current Protocols in Neuroscience*. doi: 10.1002/0471142301.ns0216s58.

Brown, C. H. *et al.* (2013) 'Physiological regulation of magnocellular neurosecretory cell activity: Integration of intrinsic, local and afferent mechanisms', *Journal of Neuroendocrinology*, 25(8), pp. 678–710. doi: 10.1111/jne.12051.

Brown, D., Fontanaud, P. and Moos, F. C. (2000) 'The variability of basal action potential firing is positively correlated with bursting in hypothalamic oxytocin neurones', *Journal of Neuroendocrinology*. doi: 10.1046/j.1365-2826.2000.00478.x.

Caldwell, H. K. *et al.* (2008) 'Vasopressin: Behavioral roles of an "original" neuropeptide', *Progress in Neurobiology*. doi: 10.1016/j.pneurobio.2007.10.007.

Caldwell, H. K. and Young, W. S. (2006) 'Oxytocin and Vasopressin: Genetics and Behavioral Implications', in *Handbook of Neurochemistry and Molecular Neurobiology*. doi: 10.1007/978-0-387-30381-9_25.

Callaway, E. M. and Luo, L. (2015) 'Monosynaptic Circuit Tracing with Glycoprotein-Deleted Rabies Viruses', *Journal of Neuroscience*. doi: 10.1523/jneurosci.0409-15.2015.

Ceccatelli, S. *et al.* (1989) 'Expression of c-Fos immunoreactivity in transmitter-characterized neurons after stress.', *Proceedings of the National Academy of Sciences*. doi: 10.1073/pnas.86.23.9569.

Cetin, A. *et al.* (2006) 'Stereotaxic gene delivery in the rodent brain.', *Nature protocols*, 1(6), pp. 3166–73. doi: 10.1038/nprot.2006.450.

Chen, P. and Hong, W. (2018) 'Neural Circuit Mechanisms of Social Behavior', *Neuron*. doi: 10.1016/j.neuron.2018.02.026.

Chini, B., Verhage, M. and Grinevich, V. (2017) 'The Action Radius of Oxytocin Release in the Mammalian CNS: From Single Vesicles to Behavior', *Trends in Pharmacological Sciences*. doi: 10.1016/j.tips.2017.08.005.

Dale, H. H. (1906) 'On some physiological actions of ergot', *The Journal of Physiology*. doi: 10.1113/jphysiol.1906.sp001148.

Dumais, K. M. *et al.* (2013) 'Sex differences in oxytocin receptor binding in forebrain regions: Correlations with social interest in brain region- and sex- specific ways', *Hormones and Behavior*. doi: 10.1016/j.yhbeh.2013.08.012.

Dumais, K. M., Alonso, A. G., Immormino, M. A., *et al.* (2016) 'Involvement of the oxytocin system in the bed nucleus of the stria terminalis in the sex-specific regulation of social recognition', *Psychoneuroendocrinology*. doi: 10.1016/j.psyneuen.2015.11.007.

Dumais, K. M., Alonso, A. G., Bredewold, R., *et al.* (2016) 'Role of the oxytocin system in

amygdala subregions in the regulation of social interest in male and female rats', *Neuroscience*. doi: 10.1016/j.neuroscience.2016.05.036.

Eliava, M. *et al.* (2016) 'A New Population of Parvocellular Oxytocin Neurons Controlling Magnocellular Neuron Activity and Inflammatory Pain Processing', *Neuron*, 89(6), pp. 1291–1304. doi: 10.1016/j.neuron.2016.01.041.

Elsabbagh, M. *et al.* (2012) 'Global Prevalence of Autism and Other Pervasive Developmental Disorders', *Autism Research*. doi: 10.1002/aur.239.

Engelmann, M. *et al.* (1998) 'Endogenous oxytocin is involved in short-term olfactory memory in female rats', *Behavioural Brain Research*. doi: 10.1016/S0166-4328(97)00084-3.

Engelmann, M. *et al.* (1999) 'Emotional stress triggers intrahypothalamic but not peripheral release of oxytocin in male rats', *Journal of Neuroendocrinology*. doi: 10.1046/j.1365-2826.1999.00403.x.

Gedeon, T., Parry, J. and Völlm, B. (2019) 'The role of oxytocin in antisocial personality disorders: A systematic review of the literature', *Frontiers in Psychiatry*. doi: 10.3389/fpsyt.2019.00076.

Grinevich, V. and Stoop, R. (2018) 'Interplay between Oxytocin and Sensory Systems in the Orchestration of Socio-Emotional Behaviors', *Neuron*. doi: 10.1016/j.neuron.2018.07.016.

Grund, T. *et al.* (2017) 'Neuropeptide S Activates Paraventricular Oxytocin Neurons to Induce Anxiolysis', *The Journal of Neuroscience*. doi: 10.1523/JNEUROSCI.2161-17.2017.

Grund, T. *et al.* (2019) 'Chemogenetic activation of oxytocin neurons: Temporal dynamics, hormonal release, and behavioral consequences', *Psychoneuroendocrinology*. doi: 10.1016/j.psyneuen.2019.03.019.

Guastella, A. J. *et al.* (2010) 'Intranasal Oxytocin Improves Emotion Recognition for Youth with Autism Spectrum Disorders', *Biological Psychiatry*. doi: 10.1016/j.biopsych.2009.09.020.

Gunaydin, L. A. *et al.* (2014) 'Natural neural projection dynamics underlying social behavior', *Cell*. doi: 10.1016/j.cell.2014.05.017.

Hasan, M. T. *et al.* (2019) 'A Fear Memory Engram and Its Plasticity in the Hypothalamic Oxytocin System', *Neuron*. doi: 10.1016/j.neuron.2019.04.029.

Hertenstein, M. J. *et al.* (2009) 'The Communication of Emotion via Touch', *Emotion*. doi: 10.1037/a0016108.

Higashida, H. *et al.* (2019) 'Social Interaction Improved by Oxytocin in the Subclass of Autism with Comorbid Intellectual Disabilities', *Diseases*. doi: 10.3390/diseases7010024.

Ho, J. M. *et al.* (2014) 'Hindbrain oxytocin receptors contribute to the effects of circulating oxytocin on food intake in male rats', *Endocrinology*. doi: 10.1210/en.2014-1148.

Hoffman, G. E. and Lyo, D. (2002) 'Anatomical markers of activity in neuroendocrine systems: Are we all "Fos-ed out"?', *Journal of Neuroendocrinology*. doi: 10.1046/j.1365-2826.2002.00775.x.

Huber, D., Veinante, P. and Stoop, R. (2005) 'Vasopressin and oxytocin excite distinct neuronal populations in the central amygdala', *Science*. doi: 10.1126/science.1105636.

Hung, L. W. *et al.* (2017) 'Gating of social reward by oxytocin in the ventral tegmental area', *Science*. doi: 10.1126/science.aan4994.

Johnson, Z. V. and Young, L. J. (2017) 'Oxytocin and vasopressin neural networks: Implications for social behavioral diversity and translational neuroscience', *Neuroscience and Biobehavioral Reviews*. doi: 10.1016/j.neubiorev.2017.01.034.

Juif, P. E. and Poisbeau, P. (2013) 'Neurohormonal effects of oxytocin and vasopressin receptor agonists on spinal pain processing in male rats', *Pain*. doi: 10.1016/j.pain.2013.05.003.

Jurek, B. and Neumann, I. D. (2018) 'The Oxytocin Receptor: From Intracellular Signaling to Behavior', *Physiological Reviews*. doi: 10.1152/physrev.00031.2017.

Kern, J. K. *et al.* (2006) 'The pattern of sensory processing abnormalities in autism', *Autism*. doi: 10.1177/1362361306066564.

Knobloch, H. S. *et al.* (2012) 'Evoked axonal oxytocin release in the central amygdala attenuates fear response', *Neuron*. Elsevier Inc., 73(3), pp. 553–566. doi: 10.1016/j.neuron.2011.11.030.

Knobloch, H. S. and Grinevich, V. (2014) 'Evolution of oxytocin pathways in the brain of vertebrates', *Frontiers in Behavioral Neuroscience*. doi: 10.3389/fnbeh.2014.00031.

Kosfeld, M. *et al.* (2005) 'Oxytocin increases trust in humans', *Nature*. doi: 10.1038/nature03701.

Köves, K. *et al.* (2012) 'Characterization of the autonomic innervation of mammary gland in lactating rats studied by retrograde transynaptic virus labeling and immunohistochemistry', *Acta Physiologica Hungarica*. doi: 10.1556/aphysiol.99.2012.2.8.

Lee, H.-J. *et al.* (2010) 'Oxytocin : the Great Facilitator of Life', *Prog. Neurobiol*, 88(2), pp. 127–151. doi: 10.1016/j.pneurobio.2009.04.001.Oxytocin.

Liu, X. *et al.* (2010) 'Association of the oxytocin receptor (OXTR) gene polymorphisms with autism spectrum disorder (ASD) in the Japanese population', *Journal of Human Genetics*. doi: 10.1038/jhg.2009.140.

LoParo, D. and Waldman, I. D. (2015) 'The oxytocin receptor gene (OXTR) is associated with autism spectrum disorder: A meta-analysis', *Molecular Psychiatry*. doi: 10.1038/mp.2014.77.

Ludwig, M. *et al.* (2002) 'Intracellular calcium stores regulate activity-dependent neuropeptide release from dendrites', *Nature*. doi: 10.1038/nature00822.

Ludwig, M. and Leng, G. (2006) 'Dendritic peptide release and peptide-dependent behaviours', *Nature Reviews Neuroscience*. doi: 10.1038/nrn1845.

M.Witt, D. (1995) 'Oxytocin and rodent sociosexual responses: from behavior to gene expression', *Neuroscience and Biobehavioral Reviews*. doi: 10.1016/0149-7634(95)00006-Z.

Mack, S. O. *et al.* (2002) 'Paraventricular oxytocin neurons are involved in neural modulation of breathing', *J Appl Physiol*. doi: 10.1152/japplphysiol.00839.2001.

Maícas-Royo, J., Leng, G. and MacGregor, D. J. (2018) 'A Predictive, Quantitative Model of Spiking Activity and Stimulus-Secretion Coupling in Oxytocin Neurons', *Endocrinology*, 159(3), pp. 1433–1452. doi: 10.1210/en.2017-03068.

Maícas Royo, J. *et al.* (2016) 'Oxytocin Neurones: Intrinsic Mechanisms Governing the Regularity of Spiking Activity', *Journal of Neuroendocrinology*. doi: 10.1111/jne.12358.

Manning, M. *et al.* (2001) 'Design of oxytocin antagonists, which are more selective than Atosiban', *Journal of Peptide Science*. doi: 10.1002/psc.339.

Marcondes, F. K., Bianchi, F. J. and Tanno, A. P. (2005) 'Determination of the estrous cycle phases of rats: some helpful considerations', *Brazilian Journal of Biology*. doi: 10.1590/s1519-69842002000400008.

Marlin, B. J. *et al.* (2015) 'Oxytocin enables maternal behaviour by balancing cortical inhibition', *Nature*. doi: 10.1038/nature14402.

McCracken J.T., et. al (2003) 'Risperidone in children with autism and serious behavioral problems.', *The Journal of pediatrics*.

Melis, M. R., Argiolas, A. and Gessa, G. L. (1986) 'Oxytocin-induced penile erection and yawning: Site of action in the brain', *Brain Research*. doi: 10.1016/0006-8993(86)91485-X.

Menon, R. *et al.* (2018) 'Oxytocin Signaling in the Lateral Septum Prevents Social Fear during Lactation', *Current Biology*. doi: 10.1016/j.cub.2018.02.044.

Nakai, J., Ohkura, M. and Imoto, K. (2001) 'A high signal-to-noise ca2+ probe composed of a single green fluorescent protein', *Nature Biotechnology*. doi: 10.1038/84397.

Netser, S. *et al.* (2017) 'A novel system for tracking social preference dynamics in mice reveals sex- and strain-specific characteristics', *Molecular Autism*. doi: 10.1186/s13229-

017-0169-1.

Neumann, I. D. *et al.* (2000) 'Brain oxytocin inhibits basal and stress-induced activity of the hypothalamo-pituitary-adrenal axis in male and female rats: Partial action within the paraventricular nucleus', *Journal of Neuroendocrinology*. doi: 10.1046/j.1365-2826.2000.00442.x.

Neumann, I. D. (2002) 'Involvement of the brain oxytocin system in stress coping: Interactions with the hypothalamo-pituitary-adrenal axis', in *Progress in Brain Research*. doi: 10.1016/S0079-6123(02)39014-9.

Neumann, I. D. (2008) 'Brain oxytocin: A key regulator of emotional and social behaviours in both females and males', *Journal of Neuroendocrinology*. doi: 10.1111/j.1365-2826.2008.01726.x.

Neumann, I. D. *et al.* (2013) 'Increased brain and plasma oxytocin after nasal and peripheral administration in rats and mice', *Psychoneuroendocrinology*. doi: 10.1016/j.psyneuen.2013.03.003.

Neumann, I. D. and Landgraf, R. (2012) 'Balance of brain oxytocin and vasopressin: Implications for anxiety, depression, and social behaviors', *Trends in Neurosciences*. Elsevier Ltd, 35(11), pp. 649–659. doi: 10.1016/j.tins.2012.08.004.

Nordmann, J. J. and Morris, J. F. (1984) 'Method for quantitating the molecular content of a subcellular organelle: hormone and neurophysin content of newly formed and aged neurosecretory granules.', *Proceedings of the National Academy of Sciences*. doi: 10.1073/pnas.81.1.180.

Oettl, L. L. *et al.* (2016) 'Oxytocin Enhances Social Recognition by Modulating Cortical Control of Early Olfactory Processing', *Neuron*. Elsevier Inc., 90(3), pp. 609–621. doi: 10.1016/j.neuron.2016.03.033.

Okamoto, Y. *et al.* (2016) 'The Potential of Nasal Oxytocin Administration for Remediation of Autism Spectrum Disorders', *CNS & Neurological Disorders - Drug Targets*. doi: 10.2174/1871527315666160413120845.

Osten, P., Grinevich, V. and Cetin, A. (2007) 'Viral vectors: A wide range of choices and high levels of service', *Handbook of Experimental Pharmacology*. doi: 10.1007/978-3-540-35109-2-8.

Owen, S. F. *et al.* (2013) 'Oxytocin enhances hippocampal spike transmission by modulating fast-spiking interneurons', *Nature*. doi: 10.1038/nature12330.

Pashaie, R. and Falk, R. (2013) 'Single optical fiber probe for fluorescence detection and optogenetic stimulation', *IEEE Transactions on Biomedical Engineering*. doi:

10.1109/TBME.2012.2221713.

Petersson, M. (2002) 'Cardiovascular effects of oxytocin', in *Progress in Brain Research*. doi: 10.1016/S0079-6123(02)39024-1.

Popik, P. and van Ree, J. M. (1991) 'Oxytocin but not vasopressin facilities social recognition following injection into the medial preoptic area of the rat brain', *European Neuropsychopharmacology*. doi: 10.1016/0924-977X(91)90010-R.

Portfors, C. V (2007) 'Types and functions of ultrasonic vocalizations in laboratory rats and mice.', *Journal of the American Association for Laboratory Animal Science : JAALAS*, 46(1), pp. 28–34. Available at: http://www.ncbi.nlm.nih.gov/pubmed/17203913.

Rash, J. A., Aguirre-Camacho, A. and Campbell, T. S. (2014) 'Oxytocin and pain: A systematic review and synthesis of findings', *Clinical Journal of Pain*. doi: 10.1097/AJP.0b013e31829f57df.

Rhodes, C. H., Morriell, J. I. and Pfaff, D. W. (1981) 'Immunohistochemical analysis of magnocellular elements in rat hypothalamus: Distribution and numbers of cells containing neurophysin, oxytocin, and vasopressin', *Journal of Comparative Neurology*. doi: 10.1002/cne.901980106.

Rossant, C. *et al.* (2015) 'Spike sorting for large, dense electrode arrays', *bioRxiv*, 19(4), p. 015198. doi: 10.1101/015198.

Rossoni, E. *et al.* (2008) 'Emergent synchronous bursting of oxytocin neuronal network', *PLoS Computational Biology*, 4(7). doi: 10.1371/journal.pcbi.1000123.

Roth, B. L. (2016) 'DREADDs for Neuroscientists', *Neuron*. doi: 10.1016/j.neuron.2016.01.040.

Rutter, L. A. *et al.* (2019) 'A Double-Blind Placebo Controlled Study of Intranasal Oxytocin's Effect on Emotion Recognition and Visual Attention in Outpatients with Emotional Disorders', *Cognitive Therapy and Research*. doi: 10.1007/s10608-018-9974-x.

Sabatier, N., Leng, G. and Menzies, J. (2013) 'Oxytocin, feeding, and satiety', *Frontiers in Endocrinology*. doi: 10.3389/fendo.2013.00035.

Sabihi, S. *et al.* (2014) 'Oxytocin in the prelimbic medial prefrontal cortex reduces anxiety-like behavior in female and male rats', *Psychoneuroendocrinology*. doi: 10.1016/j.psyneuen.2014.03.009.

Sagar, S. M., Sharp, F. R. and Curran, T. (1988) 'Expression of c-fos protein in brain: Metabolic mapping at the cellular level', *Science Science*. doi: 10.1126/science.3131879.

Sanchez-Andrade, G. and Kendrick, K. M. (2008) 'The main olfactory system and social learning in mammals', *Behavioural Brain Research*. doi: 10.1016/j.bbr.2008.12.021.

Skinner, J. A. *et al.* (2019) 'The relationship between oxytocin, dietary intake and feeding: A systematic review and meta-analysis of studies in mice and rats', *Frontiers in Neuroendocrinology*. doi: 10.1016/j.yfrne.2018.09.002.

Smith, A. S. *et al.* (2016) 'Targeted activation of the hippocampal CA2 area strongly enhances social memory', *Molecular Psychiatry*. doi: 10.1038/mp.2015.189.

Stock, S. and Uvnäs-Morbeg, K. (1988) 'Increased plasma levels of oxytocin in response to afferent electrical stimulation of the sciatic and vagal nerves and in response to touch and pinch in anaesthetized rats', *Acta Physiologica Scandinavica*. doi: 10.1111/j.1748-1716.1988.tb08294.x.

Stoop, R. (2012) 'Neuromodulation by Oxytocin and Vasopressin', *Neuron*. doi: 10.1016/j.neuron.2012.09.025.

Stoop, R., Hegoburu, C. and van den Burg, E. (2015) 'New Opportunities in Vasopressin and Oxytocin Research: A Perspective from the Amygdala', *Annual Review of Neuroscience*. doi: 10.1146/annurev-neuro-071714-033904.

Sue Carter, C. (1998) 'Neuroendocrine perspectives on social attachment and love', in *Psychoneuroendocrinology*. doi: 10.1016/S0306-4530(98)00055-9.

Swanson, L. W. and Kuypers, H. G. J. M. (1980) 'The paraventricular nucleus of the hypothalamus: Cytoarchitectonic subdivisions and organization of projections to the pituitary, dorsal vagal complex, and spinal cord as demonstrated by retrograde fluorescence double-labeling methods', *Journal of Comparative Neurology*. doi: 10.1002/cne.901940306.

Swanson, L. W. and Sawchenko, P. E. (1980) 'Paraventricular nucleus: A site for the integration of neuroendocrine and autonomic mechanisms', *Neuroendocrinology*. doi: 10.1159/000123111.

Tang, Y. *et al.* (2016) 'Distinct Types of Feeding Related Neurons in Mouse Hypothalamus', *Frontiers in Behavioral Neuroscience*. doi: 10.3389/fnbeh.2016.00091.

Tian, L. *et al.* (2009) 'Imaging neural activity in worms, flies and mice with improved GCaMP calcium indicators', *Nature Methods*. doi: 10.1038/nmeth.1398.

Tobin, V., Leng, G. and Ludwig, M. (2012) 'The involvement of actin, calcium channels and exocytosis proteins in somato-dendritic oxytocin and vasopressin release', *Frontiers in Physiology*. doi: 10.3389/fphys.2012.00261.

Tribollet, E., Barberis, C. and Arsenijevic, Y. (1997) 'Distribution of vasopressin and oxytocin receptors in the rat spinal cord: Sex-related differences and effect of castration in pudendal motor nuclei', *Neuroscience*. doi: 10.1016/S0306-4522(96)00591-X.

Uvnäs-Moberg, K., Handlin, L. and Petersson, M. (2015) 'Self-soothing behaviors with

particular reference to oxytocin release induced by non-noxious sensory stimulation', *Frontiers in Psychology*. doi: 10.3389/fpsyg.2014.01529.

Veenema, A. H. and Neumann, I. D. (2008) 'Central vasopressin and oxytocin release: regulation of complex social behaviours', *Progress in Brain Research*, 170(08), pp. 261–276. doi: 10.1016/S0079-6123(08)00422-6.

Veening, J. G. and Olivier, B. (2013) 'Intranasal administration of oxytocin: Behavioral and clinical effects, a review', *Neuroscience and Biobehavioral Reviews*. doi: 10.1016/j.neubiorev.2013.04.012.

du Vigneaud, V. *et al.* (1954) 'The Synthesis of Oxytocin 1', *Journal of the American Chemical Society*. doi: 10.1021/ja01641a004.

Wacker, D. W. and Ludwig, M. (2012) 'Vasopressin, oxytocin, and social odor recognition', *Hormones and Behavior*. doi: 10.1016/j.yhbeh.2011.08.014.

Walker, S. C. *et al.* (2017) 'C-tactile afferents: Cutaneous mediators of oxytocin release during affiliative tactile interactions?', *Neuropeptides*. doi: 10.1016/j.npep.2017.01.001.

Watanabe, T. *et al.* (2014) 'Mitigation of sociocommunicational deficits of autism through oxytocin-induced recovery of medial prefrontal activity a randomized trial', *JAMA Psychiatry*. doi: 10.1001/jamapsychiatry.2013.3181.

Weston, C. S. E. (2019) 'Four Social Brain Regions, Their Dysfunctions, and Sequelae, Extensively Explain Autism Spectrum Disorder Symptomatology', *Brain Sciences*, 9(6), p. 130. doi: 10.3390/brainsci9060130.

Wrobel, L. J. *et al.* (2010) 'Oxytocin and vasopressin enhance synaptic transmission in the hypoglossal motor nucleus of young rats by acting on distinct receptor types', *Neuroscience*. doi: 10.1016/j.neuroscience.2009.11.001.

Yizhar, O. *et al.* (2011) 'Optogenetics in Neural Systems', *Neuron*. doi: 10.1016/j.neuron.2011.06.004.

Zhang, J. B. *et al.* (2016) 'Oxytocin is implicated in social memory deficits induced by early sensory deprivation in mice', *Molecular Brain*. doi: 10.1186/s13041-016-0278-3.

Acknowledgments

I would like to sincerely thank all the people that supported me over the course of my PhD studies and contributed one way or another to the realization of this work and to the writing of this thesis.

First of all, I would like to thank Prof. Dr. Valery Grinevich for giving me the opportunity to work on this exciting project. I am very grateful for his mentoring, guidance, and support in this journey with uncountable scientific discussions, insightful comments, helpful advices, but also hard questions that incented me to explore different angles of my research.

A heartfelt thank you to all my lab members for providing a friendly environment and warm atmosphere in the lab and for helping me, whenever I needed support. A special thanks goes to Dr. Yan Tang (aka Flame), with whom I work on this project since my very first day in the lab and who shared with me his amazing experience in electrophysiology. I can't thank enough all the people I used to work with: Ferdinand, Miriam, Niki, and Judith; all the people I am still working side by side with: Marina, Ana, Arthur, Lara, Jonas and Julia. They all helped me in so many circumstances and I am grateful for that.

I would like to thank my parents, my family, and all my friends for the spiritual support, the patience, and for motivating me throughout my PhD studies and in my life in general.

Last but not least, I would like to thank my lovely girlfriend Ainhoa, who always supported and encouraged me throughout my doctoral studies.

Heidelberg, 25.06.2019